Bulletin of the Geological Survey of Japan, vol.48(6), p.313-337, 1997

Offscraping, underplating and out-of-sequence thrusting process of an accretionary prism: On-land example from the Mino-Tamba Belt, central Japan

Katsumi KIMURA*

KIMURA Katsumi (1997) Offscraping, underplating and out-of-sequence thrusting process of an accretionary prism: On-land example from the Mino-Tamba Belt, central Japan. *Bull. Geol. Surv. Japan*, vol. 48(6), p. 313-337, 22figs

Abstract: The Inuyama Sequence, a coherent Jurassic chert-clastic unit in the Mino-Tamba Belt, central Japan, represents structural styles characteristic of accretionary processes at a shallow structural level. It is characterized by a series of regional-scale thrust sheets, which form a south-verging imbricate structure asymptotically converging down into the master sole thrust of the Inuyama Sequence. Each thrust sheet, consisting of an Early Triassic to Late Jurassic oceanic plate stratigraphy, is further subdivided into an upper sheet and a lower sheet by an intrasheet detachment along the hemipelagic interval. The upper sheet is characterized by a homoclinal structure with imbricate thrusts rooted into the intrasheet detachment, while the lower sheet is characterized by the development of duplex structures and mesoscopic F_1 folds. Slip vectors from all kinds of thrusts, corrected for tectonic rotation, are directed between SSE and SSW with respect to the N60° E regional trend of the Inuyama Sequence.

The structural process of accretion can be resolved into the following four stages; (1) Formation of a decollement zone was initiated within the hemipelagic horizon, and the stratigraphic section above the decollement was progressively offscraped by in-sequence thrusting on the toe of the accretionary prism. This offscraping process was followed by (2) underplating of hemipelagic and pelagic intervals to the base of the prism in the form of duplexes with F_1 folds. This deformed section got a secondary thickening by (3) later-stage imbricate thrusting due to the reactivation of some in-sequence thrusts and their extension to the decollement, resulting in the formation of a series of regional-scale thrust sheets. Finally, (4) these imbricated thrust sheets were uplifted over a younger accreted section by out-of-sequence thrusting, leading to substantial thickening of the wedge.

1. Introduction

Seismic reflection profiles and drilling results from modern accretionary prisms suggest three structural processes characteristic of the prism growth: offscraping of incoming sediments at the toe of prisms, underplated by which material is transferred to the base of prisms, and out-of-sequence thrusting which causes substantial thickening of prisms arcward of the toe (e.g. Moore *et al.*, 1982; Kagami *et al.*, 1983; Moore *et al.*, 1985; Silver *et al.*, 1985; Westbrook *et al.*, 1988). Among these, the offscraping process, characterized by an imbricate fan structure and a basal decollement, is clearly demonstrated by seismic reflection profiles in many accretionary prisms, including the Barbados (Westbrook *et al.*, 1988; Shipley *et al.*, 1994), Nankai (Aoki *et al.*, 1982; Moore *et al.*, 1990) and Middle America (Watkins *et al.*, 1982). However, the other two processes have not been well documented by studies of modern accretionary prisms, because seismic resolution rapidly decreases arcward of the deformation front. In contrast, on-land exposed accretionary complexes, easier to observe in field, commonly represent more complicated fold-thrust structures and stratal disruption, which resulted from the overall accretionary processes. A few studies of such exposed complexes have succeeded in demonstrating the detailed geometric style and strain history of regional-scale duplexes due to underplating (e.g. Sample and Fisher, 1986; Murata, 1991; Tokunaga, 1992), and major out-of-sequence thrusts truncating previously deformed sections (Platt *et al.*, 1988; DiTullio and Byrne, 1990).

A part of the Jurassic Mino-Tamba Belt, cen-

*Geology Department, GSJ

Keywords: Mino-Tamba Belt, chert-clastic unit, Jurassic, accretionary prism, offscraping, underplating, imbricate structure, out-of-sequence thrust, decollemant, duplex.

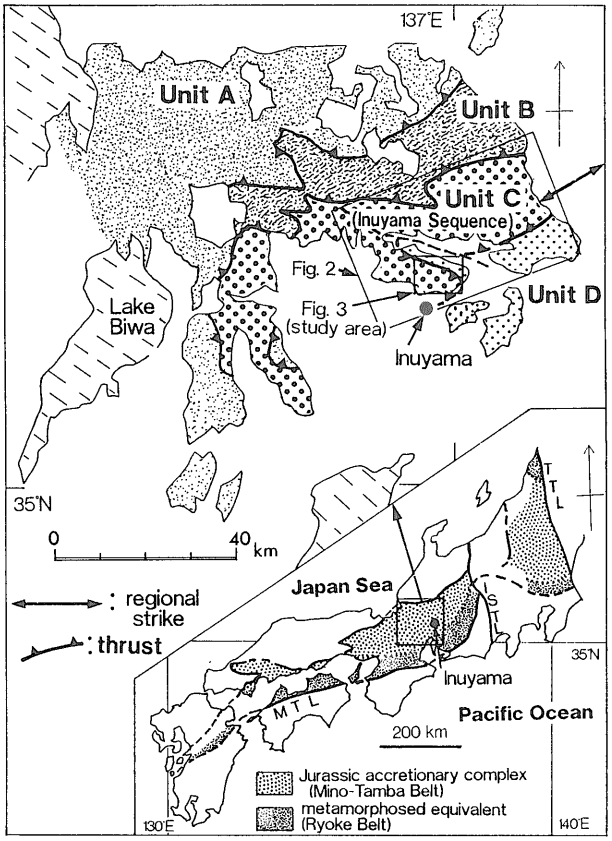

Fig. 1 Geologic divisions of the Mino-Tamba Belt into units labeled A, B, C and D, with the distribution of Jurassic accretionary complexes in the Inner zone of Southwest Japan (inset). The classification of tectonic units in the Mino-Tamba Belt is modified from Wakita (1988) and Otsuka (1988). In the inset, MTL means the Median Tectonic Line, ISTL the Itoigawa-Shizuoka Tectonic Line, and TTL the Tanakura Tectonic Line.

tral Japan, the coherent chert-clastic unit described here (Fig. 1), allows us to construct a series of accretionary processes at a shallow structural level, including offscraping, underplating and out-of-sequence thrusting. The distinct lithologies of this oceanic plate stratigraphic succession and detailed biostratigraphic data from previous studies (Yao *et al.*, 1980; Matsuda and Isozaki, 1991) help in defining regional-scale imbricate structures in the Inuyama Sequence. Metamorphic studies indicate that the sequence was accreted at a shallow level and not buried deeper than the depth of prehnite-pumpellyite facies (Hashimoto and Saito, 1970; Matsuda and Isozaki, 1991; Kimura and Hori, 1993). Kimura and Hori (1993) described the geometry of regional-scale imbricate structures based on a detailed biostratigraphic and structural analysis, and proposed a development history consisting of offscraping followed by underplating and out-of-sequence thrusting.

In this paper, I present a new detailed description, including data on the structural geometry and kinematics of duplex structures and out-of-sequence thrusts in the Inuyama Sequence, and offer a model of structural evolution of coherent accretionary unit at a shallow level.

2. Outline of Geology

2.1 Mino-Tamba Belt

The Japanese Islands had constituted a part of the eastern margin of the Asian continent before the opening of the Japan Sea in Miocene time (Otofuji *et al.*, 1985). The islands recorded continental growth due to the formation of accretionary complexes ranging in age from Paleozoic to Miocene (Kanmera, 1980). The pre-Jurassic, Jurassic and Cretaceous to Miocene accretionary complexes are arranged parallel to each other, with decreasing age from the continental side to the oceanic side (e.g. Ichikawa, 1990).

The Mino-Tamba Belt, exposed in the Inner Zone of Southwest Japan (inset of Fig. 1), is characterized by non- or weakly-metamorphosed Jurassic accretionary complexes which consist of Late Triassic to earliest Cretaceous terrigenous clastic rocks interbedded with older oceanic materials, including basalt, ribbon chert and limestone, ranging in age mainly from Carboniferous to Triassic (e.g. Mizutani, 1990).

The Mino-Tamba Belt in central Japan is divided into four tectonostratigraphic units, labeled A, B, C and D from north to south (Fig. 1). These units are separated by north-dipping thrust faults, and are arranged parallel to each other with younger units exposed toward south (Otsuka, 1988; Wakita, 1988).

Unit A includes the Sakamoto-toge, Samondake and Hunabuse units of Wakita (1988), and it consists dominantly of melange, including Carboniferous to Triassic oceanic materials such as basalt, chert and limestone, and Early to Middle Jurassic clastic rocks. Unit B comprises the Nabi and Kanayama units of Wakita (1988) and it is characterized by melange containing Triassic to Middle Jurassic chert and Middle Jurassic to earliest Cretaceous clastic rocks. Unit C, called the Inuyama Sequence (Kimura and Hori, 1993), corresponds to the northern part of the Kamiaso unit of Wakita (1988) and the complex 3 of Otsuka (1988). It is a coherent sedimentary body characterized by a series of stacked thrust sheets comprising an Early Triassic to early Late Jurassic oceanic plate stratigraphy. Unit D, which is equivalent to the complex 5 of Otsuka (1988) and the southern part of the Kamiaso unit

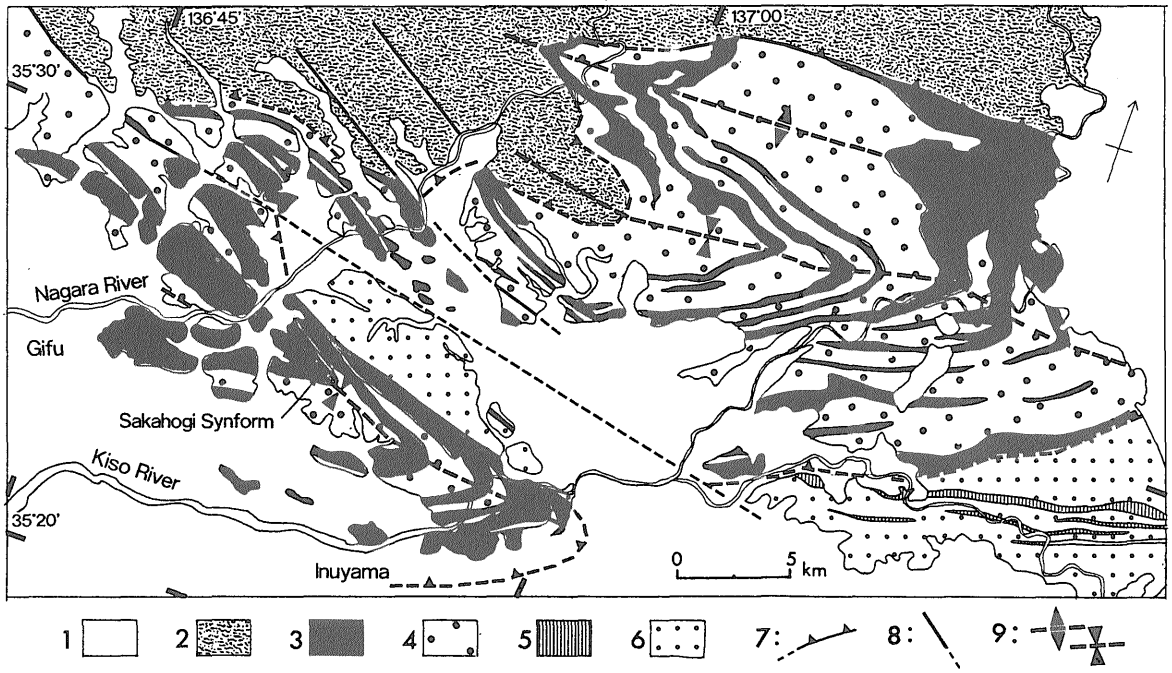

Fig. 2 Simplified map of the Inuyama Sequence in the Inuyama and nearby area. Compiled from Wakita *et al.* (1992), Yamada and Wakita (1990), and Kimura and Hori (1993).
1: cover rocks including Neogene to Quaternary sediments and Late Cretaceous igneous rocks, 2: Unit B consisting of melange including blocks of chert, 3 and 4: Inuyama Sequence (3: ribbon chert and siliceous claystone, 4: clastic rocks), 5 and 6: Unit D (5: ribbon chert, 6: clastic rocks), 7: thrust faults and inferred ones, 8: strike-slip faults and inferred ones, 9: antiform and synform. See Fig. 1 for location.

of Wakita (1988), is a coherent sedimentary body mainly consisting of the Late Jurassic sandstone and mudstone intercalated with chert. The relationship between clastic rocks and chert in this unit is not clear.

2.2 Inuyama Sequence

2.2.1 Geology

In this paper, it is described in detail and called the Inuyama Sequence after Kimura and Hori (1993).

The Inuyama Sequence has a regional trend of N60° E (Fig. 1) and dips steeply northward, with large-scale west-plunging upright folds such as the Sakahogi Synform in the Inuyama area (Figs. 2 and 3). The regional trend is judged from an enveloping surface of the upright folds. The Sakahogi Synform plunges 78° to N82° W (Kimura and Hori, 1993). Some WNW- to NW-trending strike-slip faults truncate obliquely the general trend of strata (Fig. 2). The sequence, approximately 7000 m in structural thickness, is composed of a large number of stacked fault slices. Among these, six regional-scale thrust sheets, labeled Sheets 1 to 6 in structurally ascending order (Fig. 3), are identified as bodies containing an almost complete stratigraphic succession of the Inuyama Sequence. The strata within the thrust sheets preserve bedding and original stratigraphic relation, although there are many thrust faults parallel roughly to layer.

The reconstructed stratigraphic succession, based on primarily detailed biostratigraphic studies, is grouped into the four lithologic units, in ascending order: siliceous claystone, ribbon chert, siliceous mudstone, and clastic rock (Fig. 4a; Kimura and Hori, 1993). The thickness of the stratigraphic section varies in each thrust sheet, and is estimated to range from 350 to 500 m. Lithologic features of the succession suggest that the lower two units, siliceous claystone and ribbon chert, are pelagic, the overlying siliceous mudstone is hemipelagic, and the uppermost unit is trench-fill interval including turbidite sandstone and associated mudstone. This stratigraphic succession is commonly interpreted to reflect migration of the depocenter from the abyssal plain to the trench floor (Matsuda and Isozaki, 1991; Kimura and Hori, 1993).

A number of sandstone dikes and sills occur in the lower mudstone subunit of the clastic rock horizon as well as near the boundary between the ribbon chert and the siliceous mudstone horizons (Fig. 4b). The origin of these dikes has recently been discussed by Kimura and Hori (1993) and

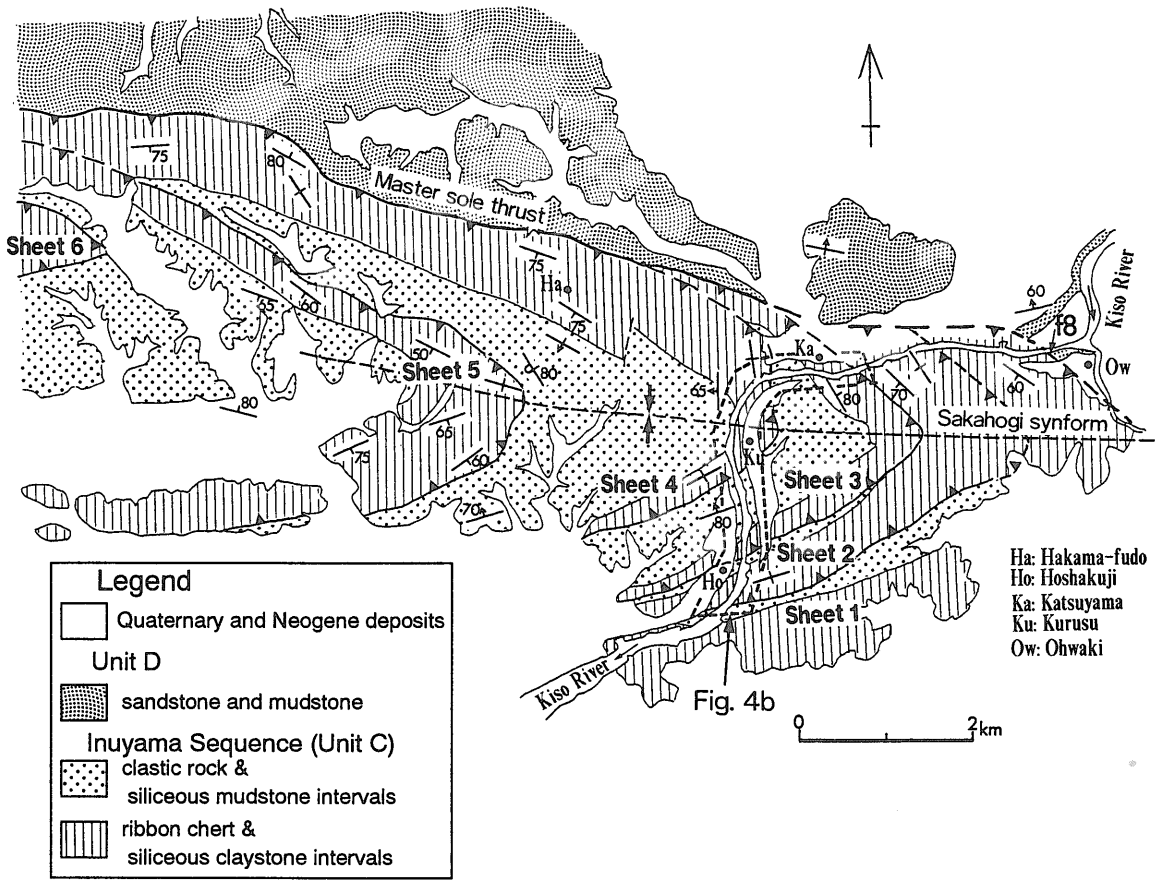

Fig. 3 Geologic map of the Inuyama Sequence of the Mino-Tamba Belt, Inuyama area, modified from Kondo and Adachi (1975). Symbol f8 shows the locality described in detail in text. See Fig. 1 for location.

Kimura (1993).

Outcrops along the course of the Kiso River provide 4 km of continuous and well exposed section striking normal to bedding. The detailed geological map there covers Sheet 2, Sheet 3 and the lower part of Sheet 4, extending from the southern limb of the Sakahogi Synform through the hinge region, into the northern limb (Fig. 4b; modified from Kimura and Hori, 1993). It is based on detailed mapping (1:2500) and biostratigraphic data from several previous studies (Yao *et al.*, 1980; Matsuda *et al.*, 1981; Mizutani and Koike, 1982; Hori, 1986, 1988, 1990; Matsuda and Isozaki, 1991; Kimura and Hori, 1993). Bedding generally strikes ENE-WSW and dips steeply north in the southern limb, and strikes NW-SE and dips 70° to 90° southwest in the northern limb of the synform (Fig. 4b).

2.2.2 Deformation history and restoration of folding and back-tilting

The deformation history of the Inuyama Sequence can be divided into two stages, both of which predate Late Cretaceous felsic volcanism (Kimura and Hori, 1993). The stage 1 displays accretion-related deformation producing south-verging thrusts and F_1 folds. F_1 folds formed in association with thrust propagation. The stage 2 is characterized by left-lateral strike-slip faults, associated with west-plunging large-scale upright folds (F_2), like the Sakahogi Synform. Upright folds (F_2) with wavelengths of 4 to 12 km occur widely in the Inner zone of Southwest Japan (Matsushita, 1953; Mizutani, 1964).

In order to determine the primary direction of accretion in a horizontal-bedding reference frame, the effects of post-accretion folding such as the Sakahogi Synform and back-tilting of the accreted units were removed using the procedure of Kimura and Hori (1993). The Sakahogi Synform is interpreted to have formed after back-tilting resulting from the stage 1 of accretion (Kimura and Hori, 1993). The effects of these deformations were removed by the following procedures: (1) Both the northern and southern limbs of the Sakahogi Synform are rotated about the synform axis with a plunge of 78° NW so that they are parallel to the N60° E regional strike of the Inuyama Sequence; (2) the bedding is rotated

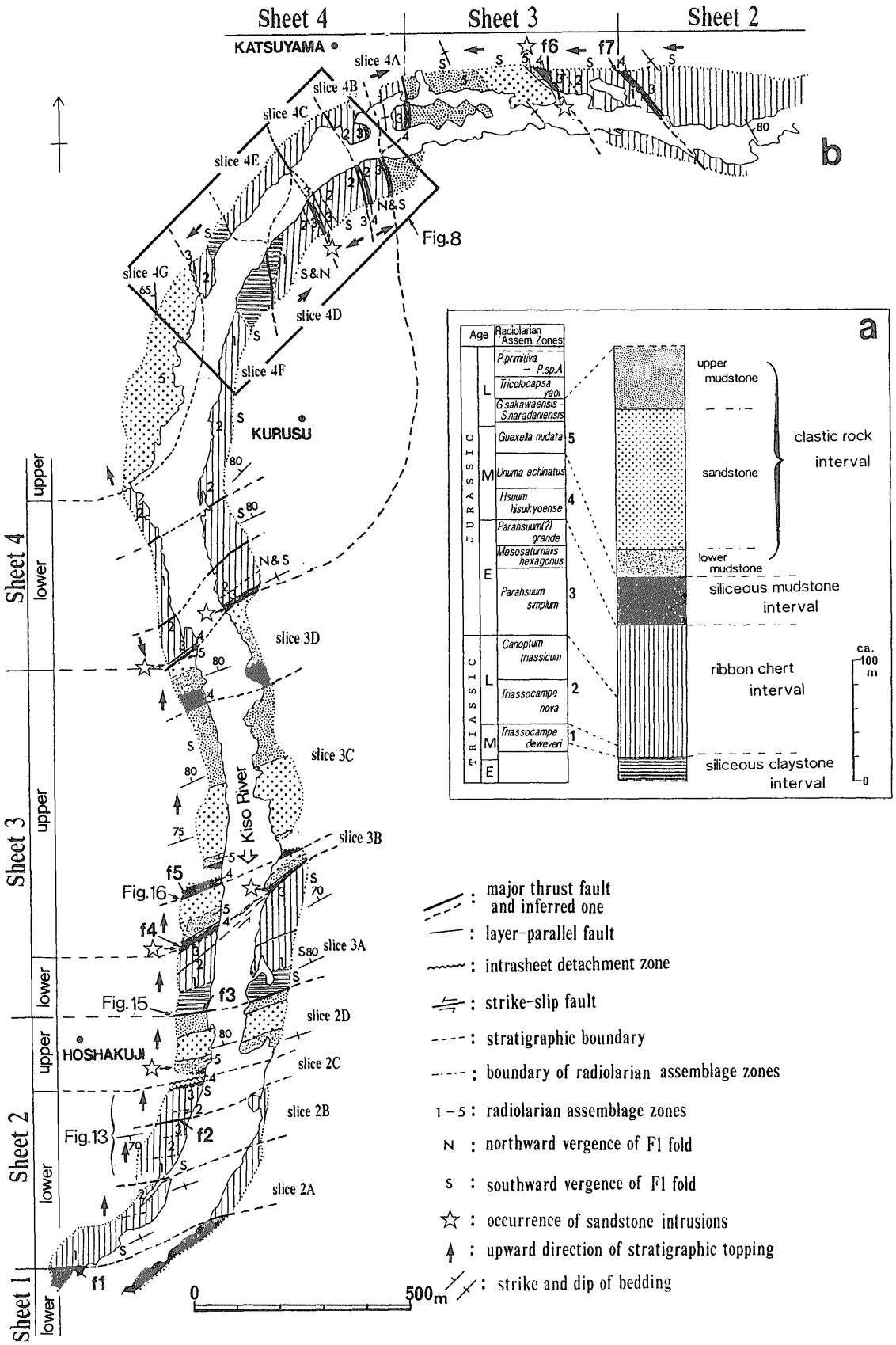

Fig. 4 a) Stratigraphic column of the Inuyama Sequence and b) geologic map along the Kiso River from Hoshakuji to Katsuyama, Gifu Prefecture (modified from Kimura and Hori, 1993).
Symbols f1 to f7 indicate the localities described in detail in text. See Fig. 3 for location.

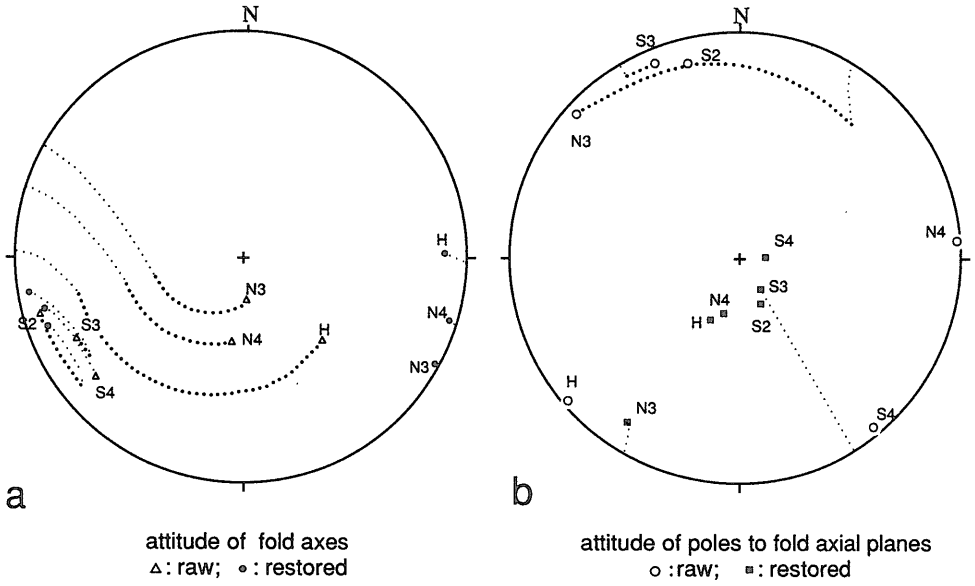

Fig. 5 Orientation of mean fold axes (a) and poles to mean axial planes (b) of mesoscopic F_1 folds in the ribbon chert and siliceous claystone intervals from each thrust sheet of the Inuyama Sequence (after Kimura and Hori, 1993). Lower-hemisphere, equal-area projection.
Raw and restored orientations are distinguished. The traces displaying two steps of procedure for restoration are shown as large dots (unfolding) and small dots (back-tilting). Refer to text for the procedure. Location of data points is given by alphabets with numbers. N and S indicate northern and southern limbs of the Sakahogi Synform, respectively, and numbers correspond to sheet numbers (2 to 4). H represents Hakama-fudo locality on Sheet 4 in the northern limb of the Synform. Numbers of folds used to calculate each mean are 34 for N3, 39 for N4, 19 for H, 38 for S2, 30 for S3 and 34 for S4, respectively. See Figs. 3 and 4b for location.

about the general strike until the bedding is horizontal.

Figure 5 indicates vector means of axes and poles to axial planes of mesoscopic F_1 folds in the ribbon chert and the siliceous claystone intervals (compiled from Fig. 15 of Kimura and Hori, 1993). The traces of restoration for folding and back-tilting are also added in Fig. 5. The fold attitudes were measured for each thrust sheet along the section in Fig. 4a and in Sheet 4 at Hakama-fudo in Fig. 3. After restoration using the procedure presented above, the resulting fabric of F_1 folds mostly shows the ENE or E-trending fold axes with southward vergence (Fig. 5), although the fabric from Sheets 3 and 4 in the northern limb of the synform indicates ESE-trending fold axes.

3. Geometry of Regional-scale Thrust Sheets

Different units of the Mino-Tamba Belt, i.e. A, B, C (Inuyama Sequence) and D, are separated by major boundary thrust faults (Fig. 1). According to detailed geological mapping (e.g. Wakita 1988 ; Kimura *et al.*, 1989), these major boundary thrusts can be traced sub-parallel to the attitude of the hanging wall units, while they crosscut internal structures of the footwall units. This relationship is also recognized in the master sole thrust of the Inuyama Sequence as described below.

The geological map from the northern limb to the hinge of the Sakahogi Synform (Fig. 3) demonstrates a SW-verging imbricate structure converging into the master sole thrust of the Inuyama Sequence. A profile section (Fig. 6) is constructed from the horizontal map view of Fig. 3, after restoration to a horizontal-bedding reference frame, and is oblique by 10° to 30° clockwise to the slip direction inferred from F_1 fold attitude of Sheets 3 and 4 in the northern limb (Fig. 5). The profile shows a flat-ramp-flat structure of Sheets 4 and 5 and constant thickness of each thrust sheet except for ramp areas.

The structural relationship between the master sole thrust and the underlying Unit D is also well exposed in this area (e.g., near Ohwaki along the Kiso River), and is described later in detail (see Fig. 3 for location). In this area, the master sole thrust is accompanied by a 200m-wide tectonic-

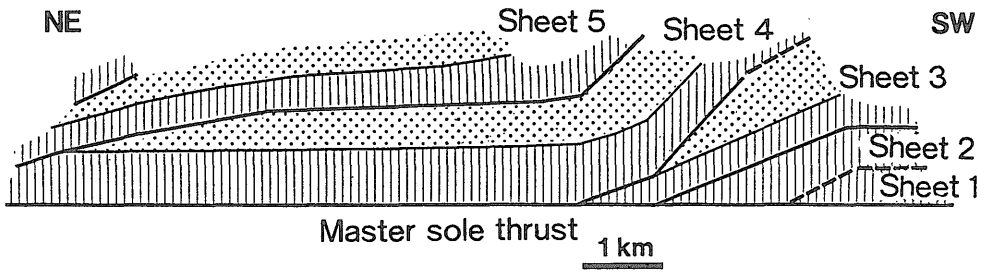

Fig. 6 Profile section of the Inuyama Sequence showing a SW-verging imbricate structure of regional-scale thrust sheets. The section is constructed from the horizontal map view of the northern limb of the Sakahogi Synform shown in Fig. 3, after correction for folding and tilting. The legend for the lithologic units is shown in Fig. 3. Modified from Kimura and Hori (1993).

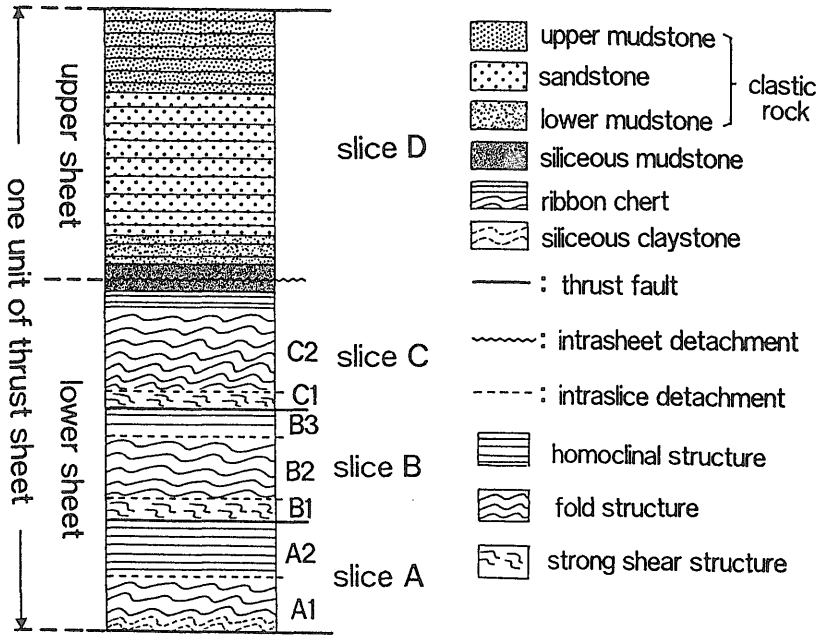

Fig. 7 Schematic diagram of internal deformational features of thrust sheets in the Inuyama Sequence (after Kimura and Hori, 1993). Each thrust sheet is divided into a lower and an upper sheets based on differences in structural style. Labels An, Bn, Cn (n=1-3) : subslices.

shear melange, whose fabric is discordant with the underlying coherent strata of the Unit D.

4. Internal Structure of Regional-scale Thrust Sheet

The internal divisions of a typical thrust sheet in the Inuyama Sequence and its associated deformation features are summarized in Fig. 7 (Kimura and Hori, 1993). A full thrust sheet is divided into a lower sheet and an upper sheet, which display major differences in structural style, and are separated by a detachment zone within the siliceous mudstone horizon (called the 'intrasheet detachment'). Both the lower and upper sheets are divisible into several slices, e.g. labeled as A, B, and C in Fig. 7, and each slice is further subdivided into subslices, e.g. labeled An, Bn, and Cn (n=1 to 3) in Fig. 7. A slice is recognized by a large structural repetition or omission of strata across its boundaries, while a subslice shows only a difference in structural style of mesoscopic F_1 folds.

4.1 The upper sheet

The upper sheet is characterized by an imbricate homoclinal structure with a few mesoscopic F_1 folds. Within this sheet, imbricated slices are commonly characterized by part of the siliceous mudstone interval with a scaly fabric at their base, as demonstrated in the upper sheet of Thrust Sheet 3 in Fig. 4b. This association sug-

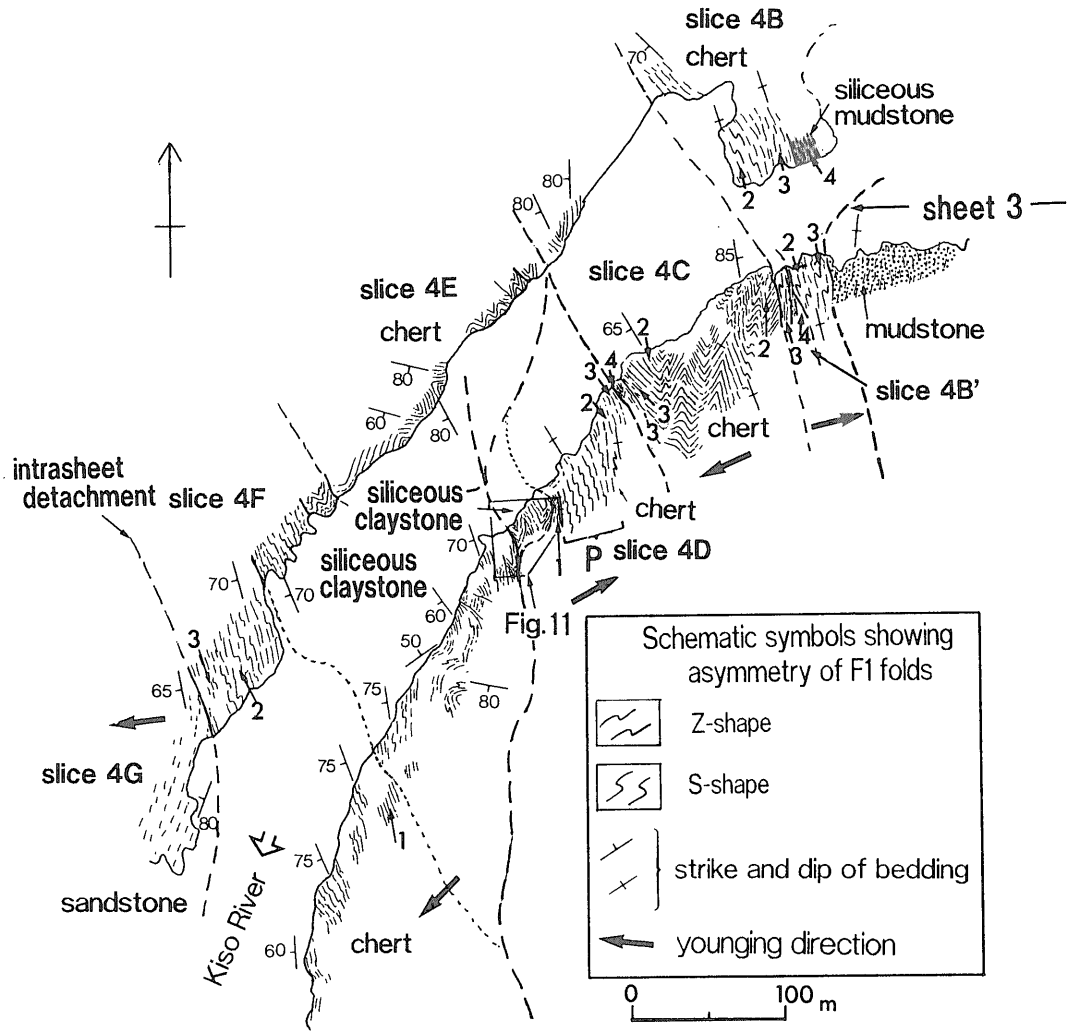

Fig. 8 Detailed sketch map of Sheet 4 in the northern limb of the Sakahogi Synform, showing bedding lines, F_1 folds, faults, and divisions of slices.
Numbers correspond to radiolarian assemblage zones (Fig. 4a), arrows indicate younging directions and symbol P indicates the locality described in detail in text. See Fig. 4b for location.

gests that these imbricate thrusts are rooted into the intrasheet detachment developed along the siliceous mudstone interval.

4.2 The lower sheet

The lower sheet generally contains several slices stacked over each other with the development of mesoscopic F_1 folds (Figs. 4b and 8), which form duplexes between the intrasheet detachment zone as a roof thrust and the basal detachment as a floor thrust as discussed later in detail. The terminology of duplex structure used in this paper is after Boyer and Elliott (1982) and McClay and Insley (1986).

Younging directions, determined by radiolarian assemblage zones in the ribbon chert and by the stratigraphic relationships, indicate that some of these slices are overturned with a width of 50 to 150 m in Sheet 4 (Figs. 4b and 8). Presence of overturned slices indicates recumbent folding associated with thrusting. Similar large recumbent folds are also present in road-cut sections through Sheet 4 near Hakama-fudo in the northern limb of the Sakahogi Synform 2 km northwest of the Kiso River section (see Fig. 3 for location).

Figure 8 shows a detailed map of the structure of the lower sheet of Sheet 4, covering a 50m-wide continuous outcrop along both sides of the Kiso River in the northern limb of the Sakahogi Synform. Along this section (Fig. 8), mesoscopic F_1 folds plunge steeply in all slices as shown in Fig. 9, the mean attitude of whose are shown as labeled N4 in Fig. 5. The slip-direction of thrusting perpendicular to these fold axes plunges 30° to 340° in the present reference frame, and hence is oblique gently to the horizontal map

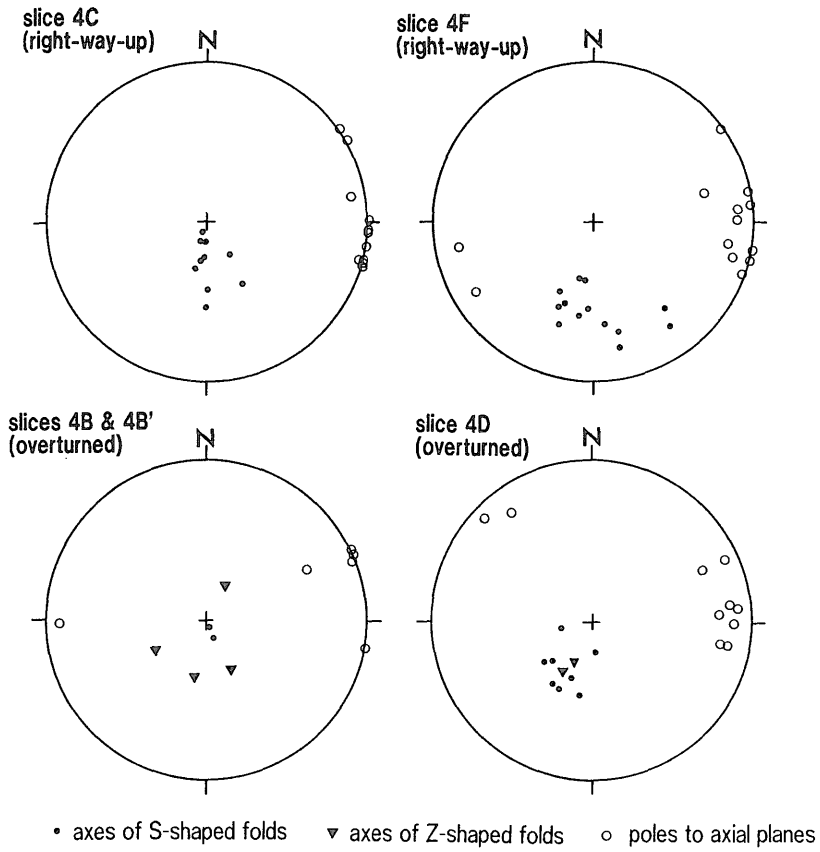

Fig. 9 Attitudes of axes and poles to axial planes of mesoscopic F_1 folds in the lower sheet of Sheet 4 in the north limb of the Sakahogi Synform. For the locations of each slice see Fig. 8. Lower-hemisphere, equal-area projection.

view of Fig. 8.

A NE-SW profile section (Fig. 10a) is constructed from the horizontal map view of Fig. 8, after restoration to a horizontal-bedding reference frame. Figure 10a displays that the lower sheet of Sheet 4 forms a large recumbent anticlinal fold consisting of two anticlines and one syncline with wavelengths of approximately 200 m. These fold structures are bounded by the overlying intrasheet detachment and underlying sole thrust. Two types of thrusts have been recognized in the lower sheet (Figs. 8 and 10a): a) the layer-parallel thrusts, and b) the low-angle thrusts. The layer-parallel thrusts bound slices and are deformed by large-scale recumbent folds, while the low-angle thrusts truncate previously folded strata (Fig. 10a).

Figure 11 displays the occurrence of a low-angle thrust, which separates slice 4D from slice 4F (see Fig. 8 for location). The low-angle thrust A clearly truncates the limb of an anticline in the hangingwall.

A restored profile section drawn in Fig. 10a implies that all axial planes of the recumbent folds are truncated by south-verging low-angle thrusts (labeled A, B, C and D in Fig. 10a). The low-angle thrust D is correlated to the sole thrust of Sheet 4 (Fig. 10a).

Figure 10b is an idealized section restored from Fig. 10a, after removing displacement along low-angle thrusts. This restoration along with the structural geometry and stratigraphic relationship shown in Figs. 8 and 10a strongly suggests that slices 4B, 4C, 4D and 4F formed a continuous folded slice before low-angle thrusting, while slice 4E, characterized by symmetric mesoscopic folds, belongs to the underlying slice. Thrust-related repetition of overturned slices 4B and 4A are too complex to be restored. The upper restored slice is estimated to be 100 to 200 m thick and more than 1500 m long from the profile section of Fig. 10b.

The enveloping surface of the restored recumbent fold dips southwestward or forward after restoration to a horizontal-bedding reference frame, where the overlying upper sheet (i.e. slice 4G) displays a homoclinal structure parallel to the intrasheet detachment (Fig. 10b). The discordant structural relationship between two restored slices of the lower sheet and the upper

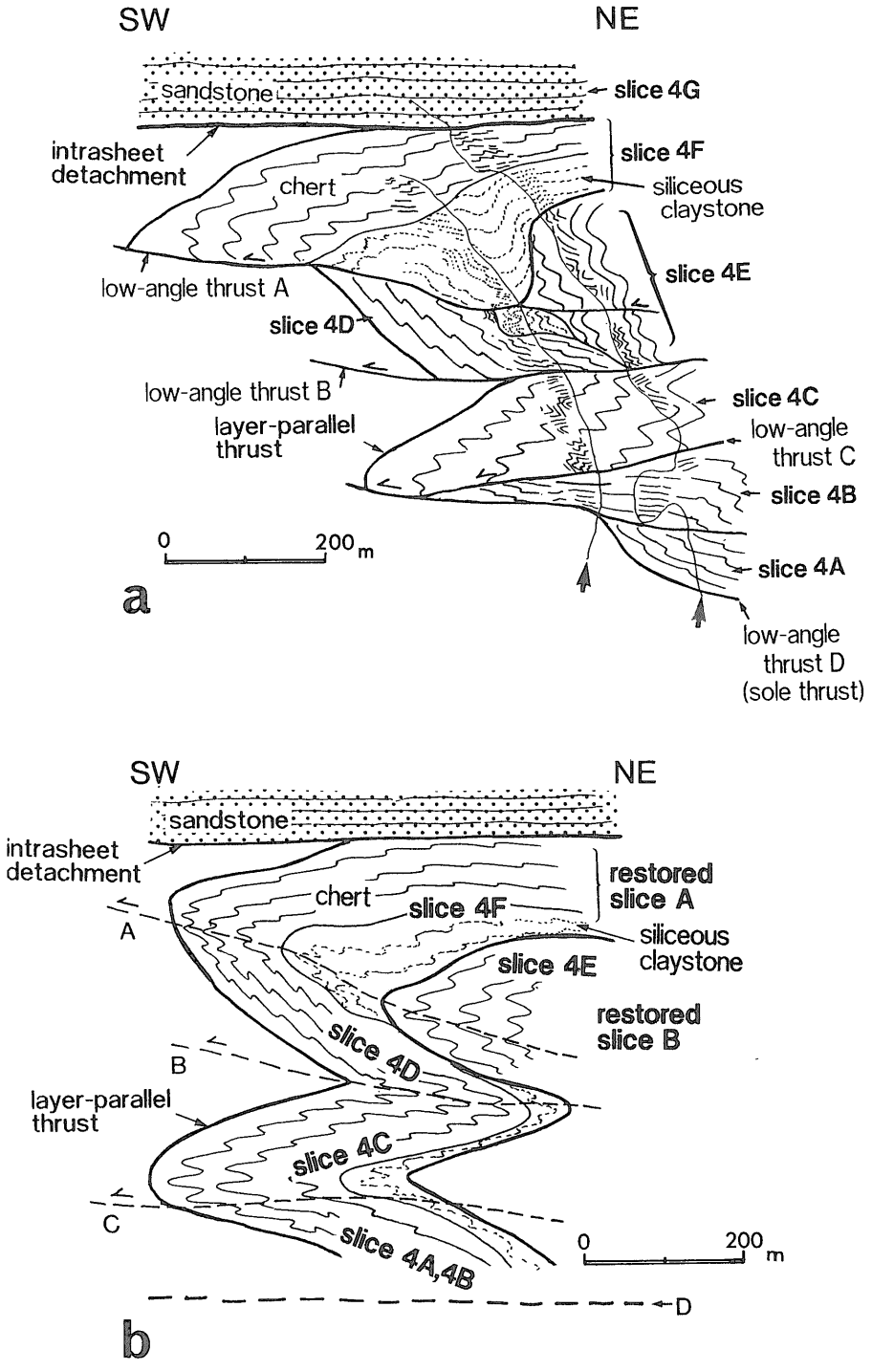

Fig. 10 (a) A profile section constructed from the sketch map in Fig. 8, corrected for folding of the Sakahogi Synform and tectonic tilting. Two thick arrows indicate the traces of the outcrop route illustrated in Fig. 8. (b) Reconstructed section before low-angle thrusting.

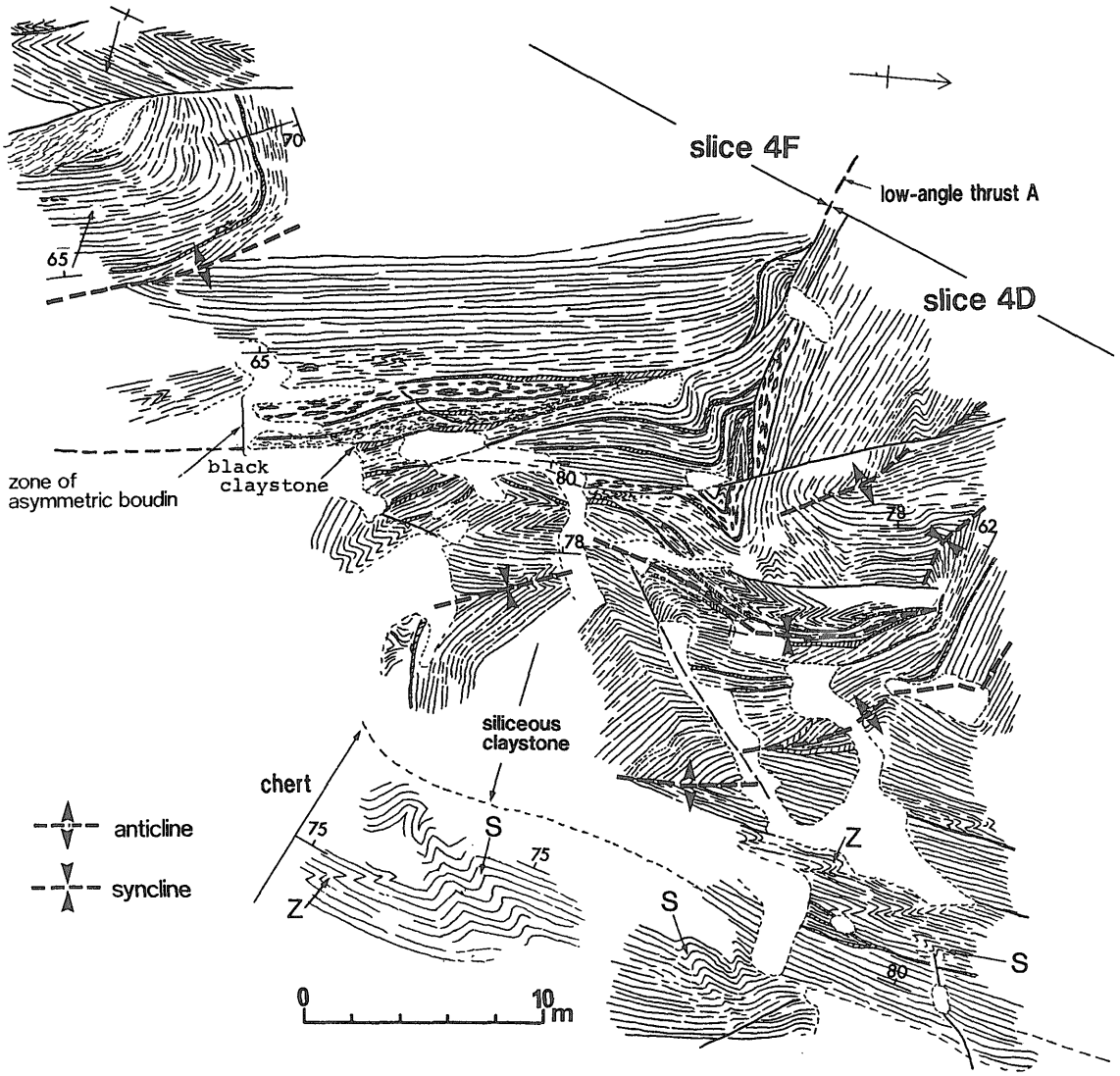

Fig. 11 Detailed horizontal sketch through the lowest part of slice 4F (right-way-up) and the lowest part of slice 4D (overturned). Axial traces indicate symmetric F_1 folds developed in the hinge area of a large-scale recumbent fold. Low-angle thrust A corresponds to a thrust having the same symbol in Figs. 8 and 10. Labels S and Z indicate S- and Z-shaped asymmetric folds, respectively. For location see Fig. 8.

sheet displays that the internal structure of the lower sheet correlates with a forward-dipping duplex overprinted by recumbent folding, which is bounded by the horizontal intrasheet detachment as a roof thrust and the sole thrust as a floor thrust.

Vergence of mesoscopic F_1 folds is useful to analyze kinematics of thrusting and recumbent folding, because F_1 folds formed not only in association with thrust propagation, but also as parasitic folds of larger-scale recumbent folds (Kimura and Hori, 1993). Vergence directions of mesoscopic F_1 folds in each slice in map view are shown in Figs. 8 and 9. S- and Z-shaped asymmetric styles of recognized folds correlate with southward and northward vergences, respectively, after restoration to a horizontal-bedding reference frame. S-shaped folds occur not only in right-way-up slices, but also in others; while Z-shaped folds occur only in overturned slices (Figs. 8 and 9). Both types of F_1 folds have parallel fold axes (Fig. 9). Symmetric F_1 folds occur frequently near the hinge areas of the larger recumbent fold (e.g. in slices 4E and the lower horizon of slice 4D in Fig. 8).

Figure 11 is a horizontal sketch, showing the occurrence of mesoscopic F_1 folds near the hinge area of a large-scale recumbent anticline (see Fig. 8 for location). Here siliceous claystones are generally characterized by the development

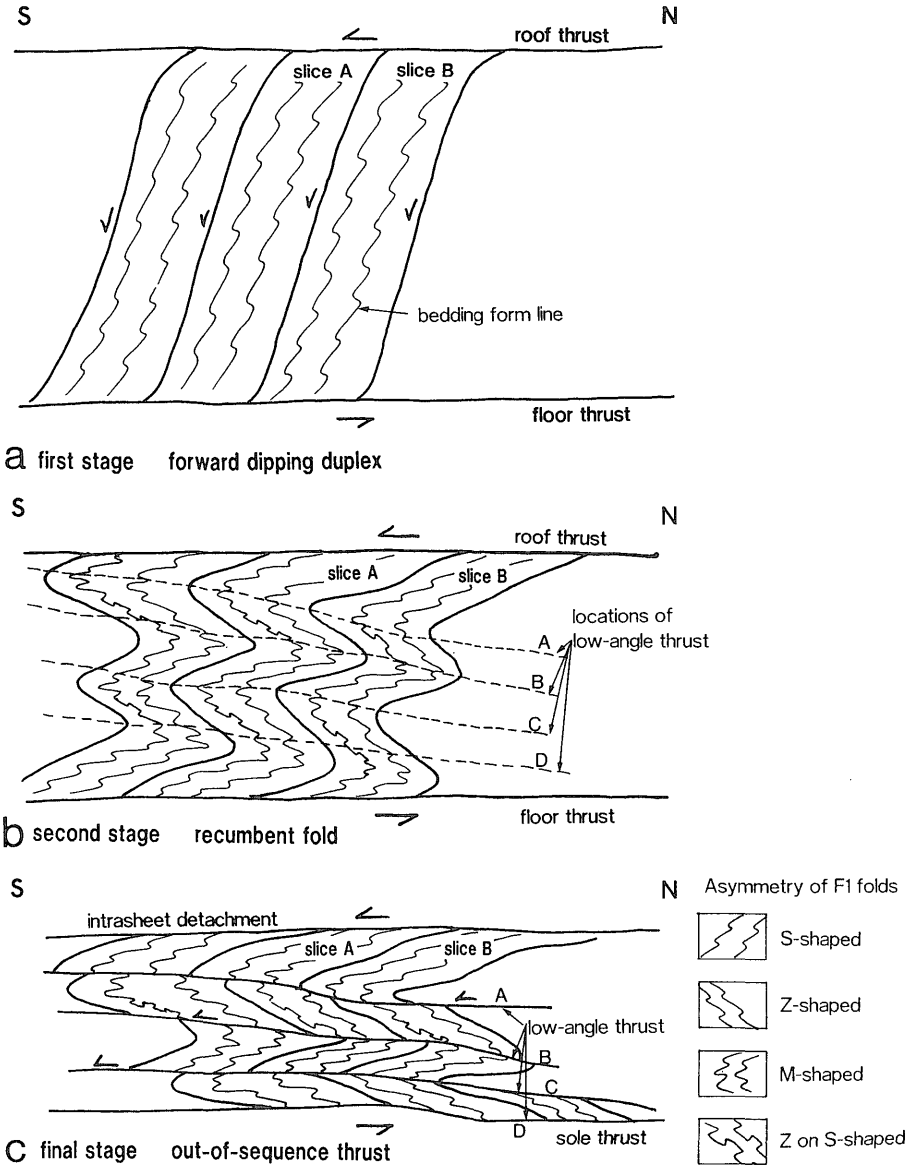

Fig. 12 Schematic cross sections (a, b and c) illustrating a progressive deformation process within the lower sheet of Sheet 4: (a) formation of a forward dipping duplex, (b) formation of a recumbent fold, and (c) truncation by low-angle thrusts as out-of-sequence thrusting.

of M-shaped symmetric mesoscopic folds, traced by thick dashed lines in Fig. 11. In contrast, the chert conformably above the siliceous claystone in overturned slice 4D is deformed by both Z- and S-shaped folds (labeled Z, S, respectively in Fig. 11).

If mesoscopic folds are associated with recumbent folding, they are expected to have S-shaped asymmetry in right-way-up slices, Z-shaped asymmetry in overturned slices, and M-shaped style in the hinge areas of recumbent folds. All but S-shaped folds in overturned slices appear to correlate with parasitic folds of large-scale recumbent folding. Although the overprinting relationship between S- and Z-shaped folds in overturned slices has not been recognized, the style and occurrence of these folds are available for estimating of the chronological relationship. S-shaped folds in overturned slices are typically developed in the 50m-thick Middle Triassic chert interval of slice 4D (locality P in Fig. 8), which is separated by a layer-parallel fault from the underlying less-deformed chert interval as shown in Fig. 11. S-shaped folds there commonly have interlimb angles ranging from 30° to 60°, half-wavelengths ranging from 50 to 150 cm and

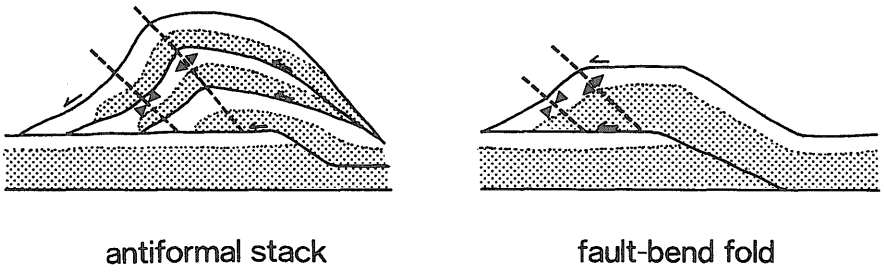

Fig. 13 Schematic structural styles of antiformal stack and fault-bend fold.

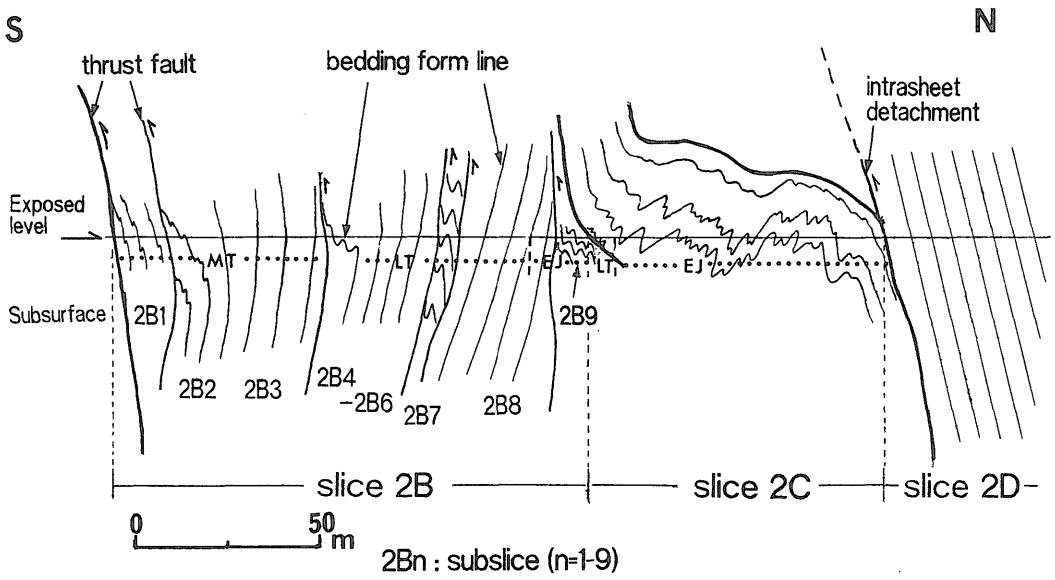

Fig. 14 Schematic cross section of slices 2B, 2C and 2D of Sheet 2 reconstructed from a detailed cross-section presented by Kimura and Hori (1993), along the west bank of the Kiso River at Hoshakuji. Slices 2B and 2C consist mainly of the ribbon chert, while slice 2D is composed of the siliceous mudstone and clastic rock. MT, LT and EJ indicate Middle Triassic, Late Triassic and Early Jurassic ages of ribbon chert, respectively. For location see Fig. 4b.

asymmetric chevron fold geometries, and gradually disappear upward. These features of folds are similar to those of F_1 mesoscopic folds developed in the same horizon of right-way-up slice. On the other hand, Z-shaped folds in overturned slices occur sporadically as drag folds associated with layer-parallel thrusting.

The different style and occurrence between S- and Z-shaped folds in overturned slices as described above suggest the following structural history of F_1 folding: (1) F_1 folds with S-shaped asymmetry were first developed in all slices in association with south-directed thrusting. They were successively followed by (2) the formation of later-stage F_1 folds such as M-shaped folds in the hinge area and Z-shaped folds in the overturned limbs as parasitic folds of recumbent folding. In right-way-up limbs, the preceding S-shaped folds are likely to have been tighter by simple shear during recumbent folding.

The above mentioned structural geometry and fabric in the lower sheet of Sheet 4 allow us to reconstruct the progressive deformation process of duplexes by shear in association with south-directed thrusting as follows (Fig. 12): (1) a foreland-dipping duplex with south-verging mesoscopic F_1 folds was initiated within the lower sheet. It was progressively overprinted by (2) large-scale recumbent folding with parasitic mesoscopic folds, and finally (3) south-verging low-angle thrusts truncated previously folded strata as out-of-sequence thrusting. The sole thrust was initiated as a floor thrust of a duplex structure and then reactivated to play an out-of-sequence thrust.

Another type of duplex structure is suggested

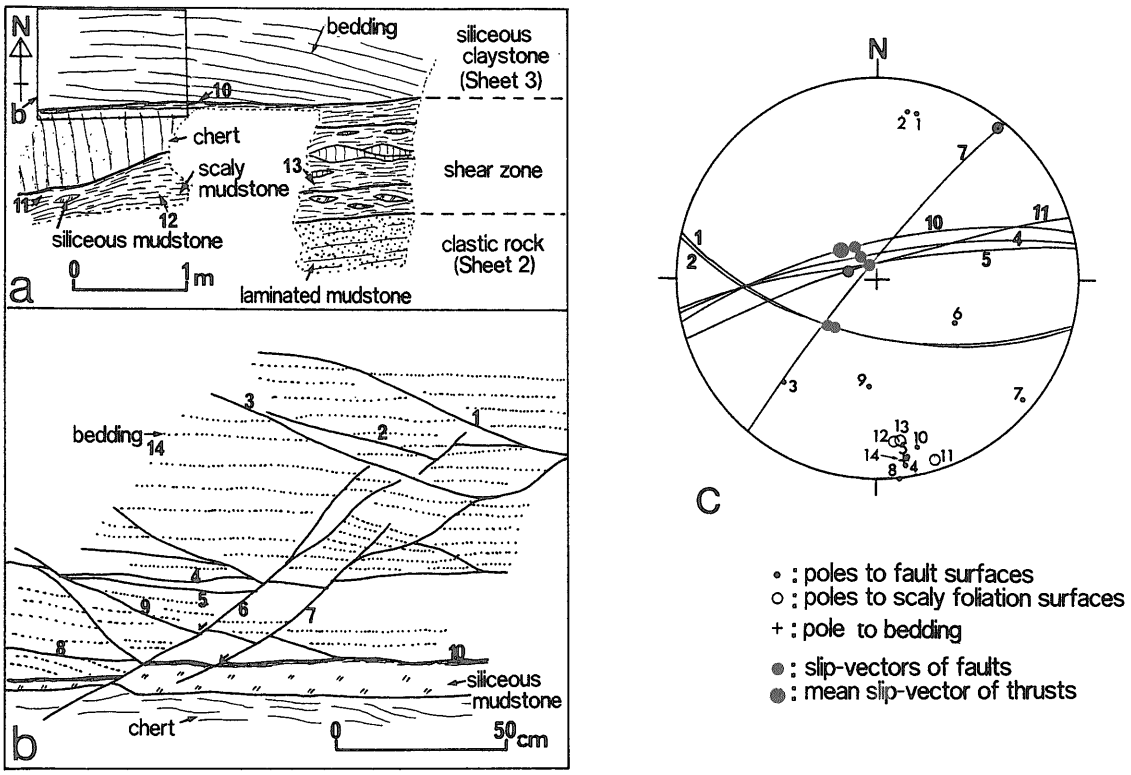

Fig. 15 (a) A horizontal section showing the sole thrust of Sheet 3 separating siliceous claystone above from underlying laminated mudstone at locality f3 (see Fig. 4b for location). (b) A detailed sketch of the hanging wall of the sole thrust showing a number of secondary shear fractures. The orientation of fractures and scaly foliation surfaces labeled by numbers 1 to 13 are plotted in (c). (c) A stereograph of fault fabric (lower-hemisphere, equal-area projection) with the orientation of slip-vectors from slickensided surfaces.

by the occurrence of anticline and syncline F_1 folds with wavelengths of 50 to 100 m recognized in slices 2A and 2B of Sheet 2 and slice 3A of Sheet 3 in the southern limb of the Sakahogi Synform (see Fig. 4b for location). Regional-scale structural geometry of this type of duplex structure parallel to the transport direction of thrust sheets cannot be observed, because all outcrops showing such structures are only in the southern limb of the Sakahogi Synform, where the horizontal terrace of outcrops is oriented perpendicular to the direction of thrusting. However, the characteristic fold style may be attributed to the forward limb of a fault-bend fold or an antiformal stack (Fig. 13).

A typical example is demonstrated by the profile section of Sheet 2 at Hoshakuji in the southern limb of the Sakahogi Synform (Fig. 14). It is a N-S-trending cross-section normal to F_1 fold axes across slices 2B, 2C and 2D of Sheet 2 (for detailed section see Fig. 8 of Kimura and Hori, 1993). Slices 2B and 2C consist mainly of the ribbon chert, and slice 2D is composed of both the siliceous mudstone and the overlying clastic rock. Slice 2C is characterized by the development of symmetric mesoscopic F_1 folds. The enveloping surface of F_1 folds in this slice forms a pair of large-scale anticlinal and synclinal folds (Fig. 14). In contrast, the overlying slice 2 D and the underlying slice 2B display a homoclinal structure with younging northward. The structural geometry of slice 2C constructed from Fig. 14, after restoration to a horizontal-bedding reference frame, corresponds to the forward limb of a fault-bend fold or an antiformal stack (Fig. 13).

5. Shear Zones and Slip-vectors of Thrust Faults

Thrust faults are commonly accompanied by shear zones with well-developed scaly foliation, ranging from several mm to 13 m in width. The master sole thrust, however, is characterized by associated broad tectonic-shear melange zone, which is 200 m wide. The width of the shear zones varies with lithology and stratigraphic

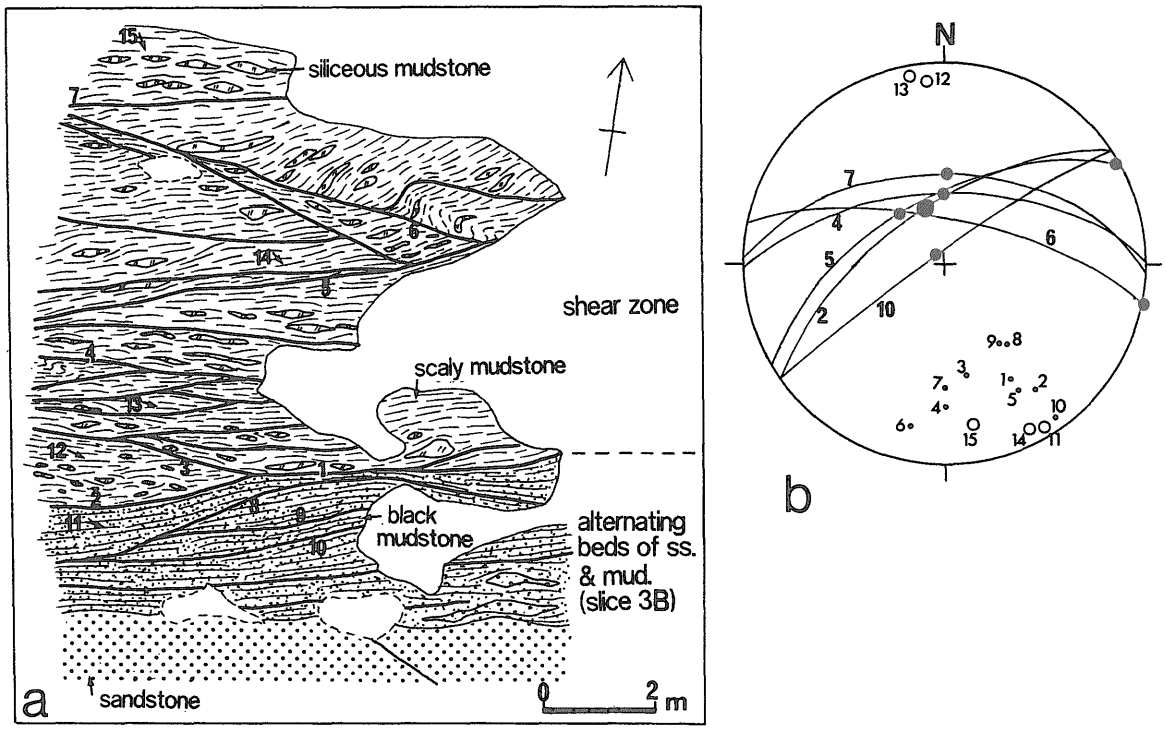

Fig. 16 (a) A horizontal sketch of the shear zone along the sole thrust of slice 3C, Sheet 3 at locality f5 (see Fig. 4b for location). The orientation of surfaces labeled by numbers 1 to 14 is plotted in (b). (b) A stereograph of fault fabric (lower-hemisphere, equal area projection). See Fig. 15 for the legend.

position, and width of greater than 1 m occurs only in the siliceous claystone and the siliceous mudstone intervals. Scaly foliations in mudstone have polished surfaces with slickenlines and form an anastomosing texture at the scale of millimeters. Thrust fault surfaces within the siliceous claystone, ribbon chert, and siliceous mudstone intervals are generally coated by mud films without any mineral veins, and those within the clastic rock are commonly filled by calcite veins. Three typical shear zones along major thrust faults, shown in Figs. 15, 16 and 17, are described below.

5.1 Shear zones of major thrust faults

5.1.1 The shear zone along the sole thrust of Sheet 3 (locality f3 in Fig. 4)

This shear zone separates the overlying siliceous claystone unit of Sheet 3 from the underlying upper mudstone subunit of Sheet 2. Along the shear zone, siliceous mudstone shows a scaly fabric with lenses of chert and massive siliceous mudstone (Fig. 15a). Slickenlines present on secondary fault surfaces within the hanging wall (Fig. 15b), on scaly foliation surfaces within the shear zone, and on the northern boundary surface of the shear zone (Figs. 15a and b) have pitches of 76° to 88° from W. The mean slip-direction is 78° from W on the boundary fault surface (Fig. 15c), which is very close to the slip-direction (85° from W) of the boundary fault (fault 10 in Fig. 15b). This thrust-related fabric is partly truncated by a NE-trending fault (fault 7) having subhorizontal slickenlines (Figs. 15b and 15c).

5.1.2 The shear zone along an imbricate thrust in the upper sheet of Sheet 3 (locality f5 in Fig. 4)

This shear zone separates the siliceous mudstone horizon of slice 3C above from the clastic rock horizon of slice 3B below, and is marked by a 13m-wide zone of siliceous mudstone with well-developed scaly foliation. Figure 16a is a horizontal section across the lower part of the shear zone. Slickenlines on secondary shear fractures or fault surfaces and on scaly foliations in the shear zone have pitches of 82° to 95° from W (Fig. 16b). The mean slip-direction is 83° from E on the boundary fault surface, which is almost equal to the slip-direction (82° from E) of the boundary fault. These thrust-related fabrics along the shear zone are also locally overprinted by left-lateral strike-slip, recognized by the presence of subhorizontal slickenlines on faults 5 and 6 and by the presence of steeply plunging S-shaped drag folds (Figs. 16a and b).

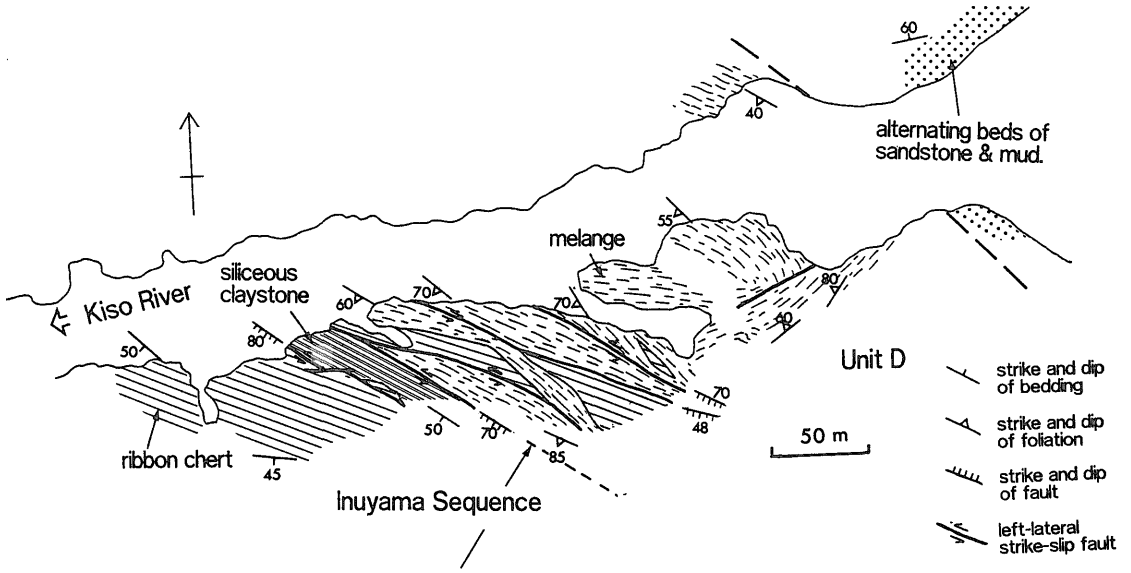

Fig. 17 Detailed geologic map of locality f8, Ohwaki (see Fig. 3 for location) showing deformation features near the master sole thrust accompanied by the melange. The melange separates the siliceous claystone of the Inuyama Sequence from the underlying alternating beds of sandstone and mudstone of the Unit D.

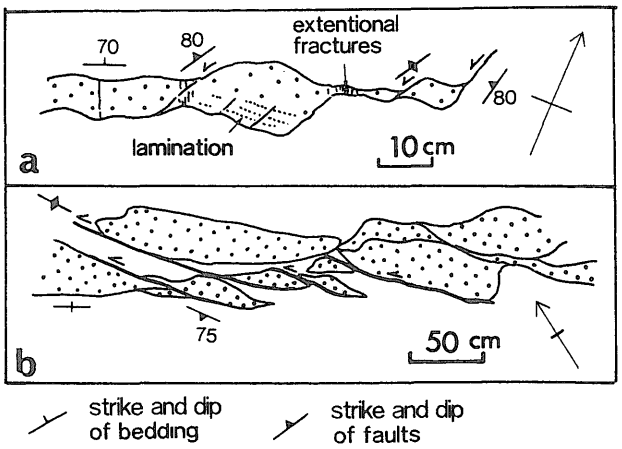

Fig. 18 Horizontal sketches from the melange zone associated with the master sole thrust of the Inuyama Sequence in Fig. 17, showing (a) pinch & swell structures in a sandstone bed associated with small-scale normal faults, and (b) imbrication of sandstone lenses suggesting contractional deformation caused by reverse faults.

5.1.3 The shear zone along the master sole thrust of the Inuyama Sequence (locality f8 in Fig. 3

The master sole thrust is accompanied by a broad shear zone consisting of a 200m-thick melange unit, which is well exposed along the river terrace of the Kiso River (Fig. 17). The melange there is overlain by the siliceous claystone horizon of Sheet 1 and underlain by alternating beds of sandstone and mudstone belonging to the Unit D. Bedding structure of the underlying alternating beds is oblique to the boundary fault between alternating beds and the melange (Fig. 17), and hence it is crosscut by the boundary fault.

The melange consists of blocks of various types of materials in a scaly mudstone matrix. The blocks are composed of sandstone, alternating beds of sandstone and mudstone, and ribbon chert with a minor amount of siliceous mudstone. Early Late Jurassic radiolarian fossils have been obtained from siliceous mudstone within the melange (Otsuka, 1988). The age of siliceous mudstone is early Middle Jurassic in the Inuyama Sequence (Fig. 4a), and late Middle to Late Jurassic in the underlying Unit D (Adachi, 1982, 1988). Therefore, the age data suggest that the melange resulted mainly from disruption and mixing of rocks in the underlying Unit D.

Blocks of sandstone contain three different kinds of deformation structures (Fig. 18), which reflect a progressive deformation process associated with thrusting. The first type of structure is pinch-and-swell, boudinage and extensional fractures filled by calcite or quartz veins (Fig. 18a). The second type of structure is asymmetric shaped sandstone blocks separated by right-stepping normal fault arrays, which are oblique to bedding and converge into bedding (Fig. 18a). The sandstone beds commonly display

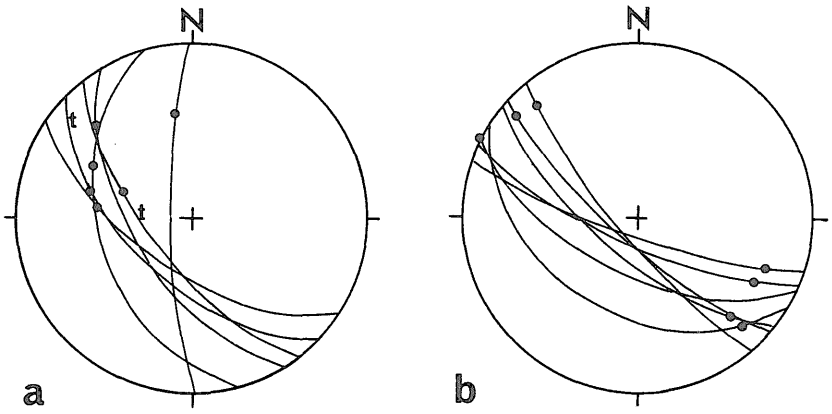

Fig. 19 Orientations of slickenlines on fault and scaly foliation surfaces from the shear zone of the master sole thrust of the Inuyama Sequence in Fig. 17; (a) Thrust faults (labeled t) and scaly foliation. (b) Strike-slip faults. Lower-hemisphere, equal-area projection.

soft deformation associated with the first and second types of structures, which reduce significantly the thickness of the sandstone beds (Fig. 18a). These two types of structures are overprinted by the third type of structure. The third type of structure represents contractional deformation caused by left-stepping reverse fault arrays, which are oblique at low angle to bedding and are filled by calcite or quartz veins (Fig. 18 b). Blocks of sandstone are commonly sheared by cataclastic deformation in association with anastomosing networks of fractures (web structure termed by Byrne, 1984).

In addition to subsidiary faults related to sandstone boudins as mentioned above, two different kinds of mesoscopic faults are distinguished in the melange and the overlying sheared siliceous claystone unit. The first type of fault is characterized by mud film-coated wavy surfaces with slickenlines, which are oriented parallel to slickenlines on scaly foliation surfaces of a mudstone matrix in the melange (Fig. 19a), having pitches ranging between 30° and 60° from NW (Fig. 19a). These orientations, after restoration to a horizontal-bedding reference frame, are consistent with the general slip-direction of thrusting (f8 in Fig. 20). These faults are also closely associated with the asymmetric arrays of sandstone boudin as mentioned above. Accordingly, these faults are regarded as south-verging thrusts. These thrusts are sometimes overprinted or crosscut by the second type of faults. The second type of fault exhibits planar fault surfaces filled with quartz and calcite veins and have nearly horizontal slickenlines (Fig. 19b). Associated drag folds and asymmetric shear fabric of scaly foliation surfaces indicate left-lateral slip. Hence, the second type of fault is regarded as a left-lateral strike-slip fault. This type of fault is particularly well developed near the boundary between the siliceous claystone and the melange units.

These structural features indicate that the melange associated with the master sole thrust at this location was produced by shear in association with south-directed thrusting, and was later overprinted by left-lateral strike-slip. In fact, asymmetric array of sandstone boudin, scaly foliation surfaces and thrust faults characteristic of the melange at this location have been recognized in many on-land exposed accretionary complexes, and are characteristic of melanges generated by tectonic-shear in association with thrusting (termed tectonic - shear melange) (Fisher and Byrne, 1987; Needam and Mackenzie, 1988; Kimura and Mukai, 1991; Kano *et al.*, 1991).

5.2 Slip-vectors of thrusting

The slip direction data were collected from major thrust faults at eight localities along the Kiso River (boundary faults between tectonic packets: localities f1-f7; the master sole thrust: locality f8; see Figs. 3 and 4 for location). The slip-direction of each fault, using the pitches of slickenlines, was measured on fault surfaces making boundaries of the shear zones along thrusts at the localities f2, f3, f4, and f5 in Fig. 4. On the thrust faults at the localities f1, f7, and f8 (Figs. 3 and 4), slickenlines on a number of subsidiary faults and scaly foliation surfaces were measured, and then their mean orientation was calculated, because slickenlines were not found on main boundary fault surfaces.

The orientation of slickenlines of the thrust faults at the localities f3 and f5, as described

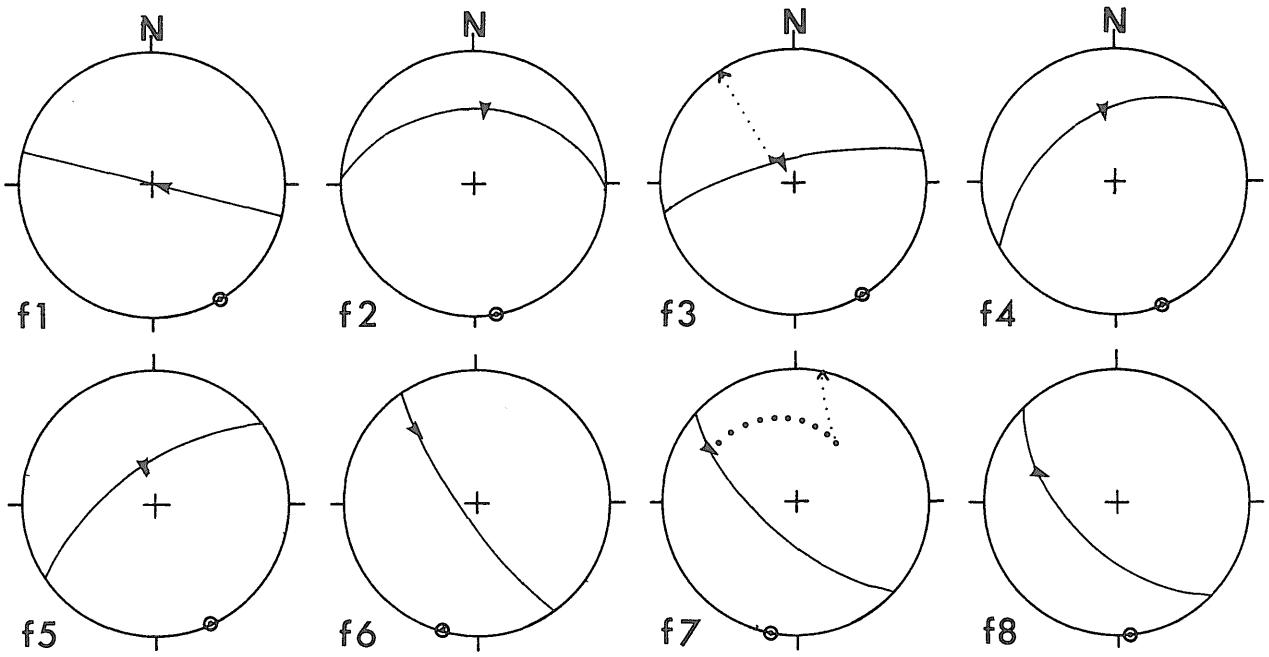

Fig. 20 Slip-direction for major thrust faults at localities f1–f8 along the Kiso River in the Inuyama area (see Figs. 3 and 4b for localities). Great circles show attitude of fault surfaces, and arrows indicate direction of slip-vectors (hangingwall-over-footwall). Double circles on peripheries of stereonets show slip-vectors after correction. The traces displaying two steps of correction for f3 and f7 are shown as large dots (unfolding) and small dots (back-tilting). Lower-hemisphere, equal-area projection.

before (see Figs. 15 and 16), were measured not only on the boundary fault surfaces, but also on the subsidiary fault surfaces. The resulting values show that the orientation of slickenlines on the both surfaces is almost equal, as shown in Figs. 15c and 16b.

On the sole thrust of Sheet 3 at the locality f6, the slip-direction was calculated from the mean direction of intersections between nine horses and a roof thrust in a mesoscopic hinterland-dipping duplex just above the shear zone.

The resulting pitches of slickenlines on the thrust fault surfaces vary between 76° to 95° from E in the southern limb, and between 26° to 42° from NW in the northern limb of the Sakahogi Synform (Fig. 20). As shown in Fig. 20, after restoration to a horizontal-bedding reference frame, the resulting slip-direction of the thrust faults trends between SSE and SSW with respect to the N60° E regional trend of the Inuyama Sequence.

The sense of fault slip was determined by microscopic to mesoscopic asymmetric scaly fabrics, including shear bands (localities f1–f5, f7 and f8), mesoscopic duplex (locality f6) and drag folds (locality f2) (see Figs. 3 and 4).These asymmetric fault fabrics indicate southward-directed slip after restoration. Accordingly, slip vectors from these different kinds of major thrusts lie between SSE and SSW in a horizontal-bedding reference frame (Fig. 20). The direction of slip vectors is also consistent with those derived from the orientations and vergence of mesoscopic F_1 folds (Fig. 5b).

6. Discussion

The overall accretionary process of the Inuyama Sequence discussed here is based on the structural features described in the previous sections. The geometrical structure and the deformation process of the Inuyama Sequence appear to be comparable to those of modern accretionary prisms. These similarities are being discussed first.

6.1 Structural features of active accretionary wedges

High-quality seismic reflection data across modern active accretionary prisms, such as the Barbados Ridge and the Nankai Trough areas, reveal a common set of thrust-related structures (e.g. Kagami, 1985; Moore *et al.*, 1985; Westbrook *et al.*, 1988; Brown *et al.*, 1990; Moore *et al.*, 1990; Shipley *et al.*, 1994). Recent studies of the frontal part of the Nankai accretionary prism reveal that these prisms can be subdivided, based on

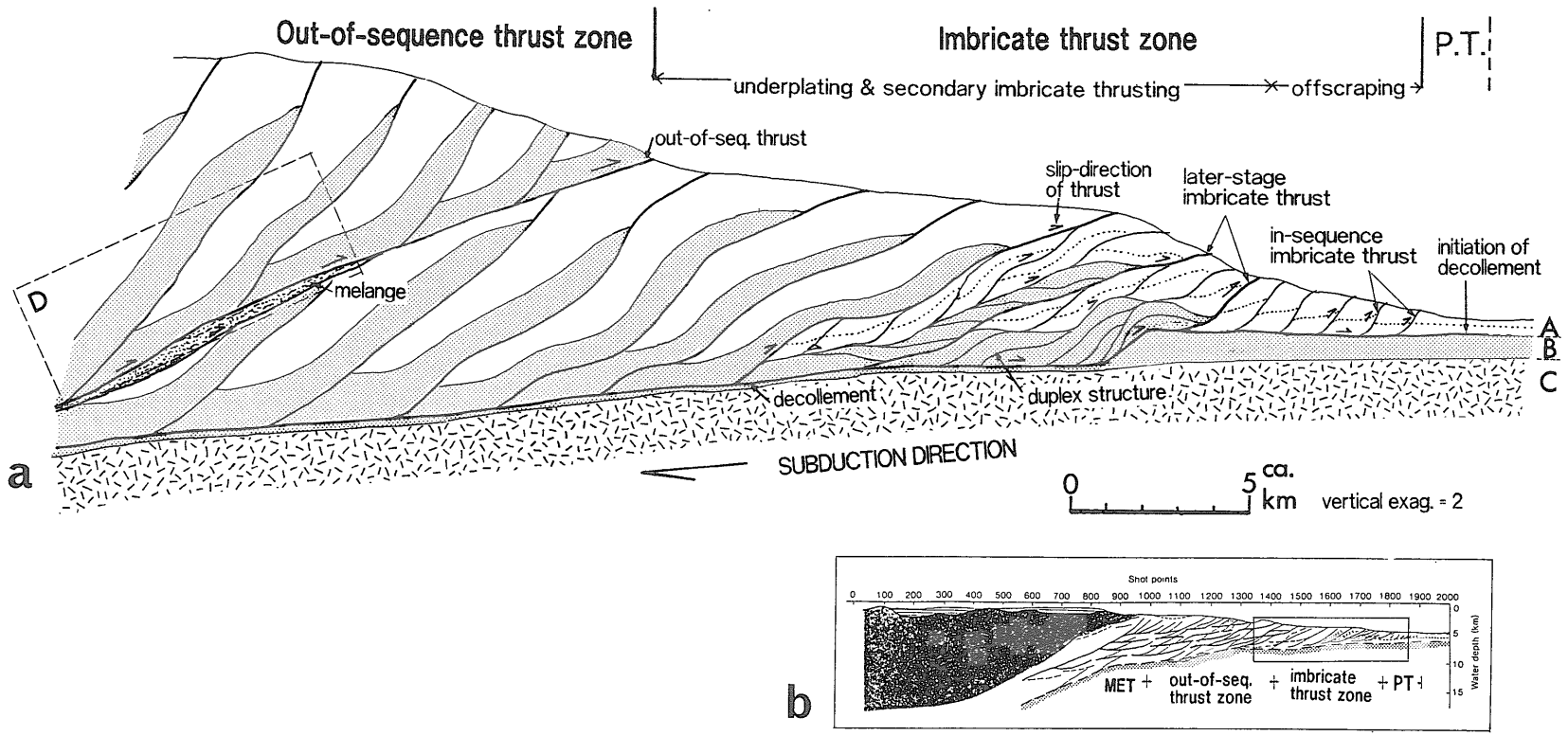

Fig. 21 (a) Schematic cross section illustrating the structural evolution of the Inuyama Sequence based on structural analysis. Note that the rectangle D may correlate to the exposed level of the Inuyama Sequence as shown in Fig. 6.
Label A: the clastic rock interval and the upper part of the siliceous mudstone interval. Label B: the lower part of the siliceous mudstone, the ribbon chert and the siliceous claystone intervals. Label C: oceanic basement which is inferred to be an oceanic crust. P.T. : protothrust zone. Dashed line in A zone: bedding form line.
(b) A cross section illustrating schematically four tectonic zones in the Nankai accretionary prism (from Kagami, 1985). The tectonic position remarked by a rectangle may correspond to the Fig. 21 (a).
PT : Protothrust zone. MET : Major earthquake thrust zone. Shot points are plotted at a distance of 5 km.

structural changes, into three tectonic zones, from seaward to landward: the protothrust zone, the imbricate thrust zone, and the out-of-sequence thrust (or multiple decollement) zone (Kagami *et al.*, 1983; Taira *et al.*, 1992) (Fig. 21b).

According to Kagami *et al.* (1983), Kagami (1985) and Taira *et al.* (1992), a brief description of each tectonic zone is as the following. The protothrust zone is located just seaward of the frontal thrust of a prism. It is characterized by development of box-folds and high-angle thrusts in the stratigraphic section above the incipient growth of a basal decollement. The imbricate thrust zone is characterized by the seaward propagation of in-sequence thrusting with a series of imbricate thrust slices. All these thrusts sole into a regional-scale decollement. A basal decollement zone separates stacked imbricate thrust sheets above from nearly undeformed sediments below. The out-of-sequence thrust zone is characterized by downward migration of the decollement zone to a deeper level and by the development of low-angle thrusts which cut the previously deformed structure of accreted sediments. As a result, the prism thickens substantially and the slope steepens relative to the other two zones. Such tectonic divisions and accretionary process are similar to other active accretionary wedges, although there are also minor differences (e.g. Moore *et al.*, 1985).

6.2 Accretionary process of the Inuyama Sequence

Figure 21a schematically illustrates accretionary processes of the Inuyama Sequence in the frontal part of an accretionary prism, which covers the protothrust, the imbricate thrust and the frontal part of the out-of-sequence zones (refer to Fig. 21b). This structural model is improved from the model presented by Kimura and Hori (1993).

Two significant geometric and kinematic constrains concerned with regional-scale structural features are derived from the Inuyama Sequence: (1) regional-scale geometry of the Inuyama Sequence displays south-verging imbricate structures converging into a master sole thrust as demonstrated in the cross-section of Fig. 6; (2) the master sole thrust truncates the underlying Unit D. These features of regional-scale thrust system correlate with the structural features of the out-of-sequence thrust zone in active wedges.

In Fig. 21a, the rectangle D, located within the out-of-sequence thrust zone, approximates the cross-section of the Inuyama Sequence shown in Fig. 6. The master sole thrust is regarded as a low-angle out-of-sequence thrust, along which the Inuyama Sequence was thrust over the younger Unit D. The master sole thrust is illustrated to have been rooted into the decollement in Fig. 21a, so that a series of thrust sheets can turn to converge into a basal decollement of a prism, as shown in Fig. 21a, after restoring the dislocation along the out-of-sequence thrust. In Fig. 21a, the decollement is inferred to have occurred within the lowest siliceous claystone interval, because the underlying rocks were separated from the accreted rocks and were not exposed. It is illustrated in Fig. 21a that oceanic crust was subducted below the decollement. The master sole thrust of the Inuyama Sequence is one of boundary faults, by which the Mino-Tamba Jurassic accretionary complex is subdivided into major tectonic units. Accordingly, the other boundary thrusts may also have been developed as major out-of-sequence thrusts of accretionary wedges.

Each thrust sheet has four types of major thrust faults, as described in the previous section: (1) the intrasheet detachment along the siliceous mudstone horizon, which subdivides each thrust sheet into a lower sheet and an upper sheet, (2) imbricate thrusts within the upper sheet, rooted into the intrasheet detachment, (3) duplex structures within the lower sheet, and (4) a sole thrust of each thrust sheet.

From comparison with structural styles and kinematics of the frontal part of an active prism, Kimura and Hori (1993) regarded the intrasheet detachment as an initial decollement zone, imbricate thrusts within the upper sheet as in-sequence thrusts at the toe of a prism, and a sole thrust as an out-of-sequence thrust in the out-of-sequence thrust zone, and attributed the formation of duplex structures to underplating at the base of a prism. This study further provided detailed geometry and kinematics of duplex structures and sole thrusts in the Inuyama Sequence. These newly obtained data allow us to clarify accretionary processes in detail.

On active wedges, although seismic reflection studies have not succeeded in revealing internal structures of underplated sections, the formation of duplexes is commonly considered to be an important mechanism for underplating in accretionary prisms (i.e. Silver *et al.*, 1985; Moore *et al.*, 1985; Sample and Fisher, 1986). This idea is supported by the presence of a few regional-scale duplex structures from on-land exposed accretionary complexes (Sample and Fisher, 1986; Murata, 1991; Tokunaga, 1992).

Geometrical features and structural fabric of duplex structure in the Inuyama Sequence, described in the previous section, have revealed

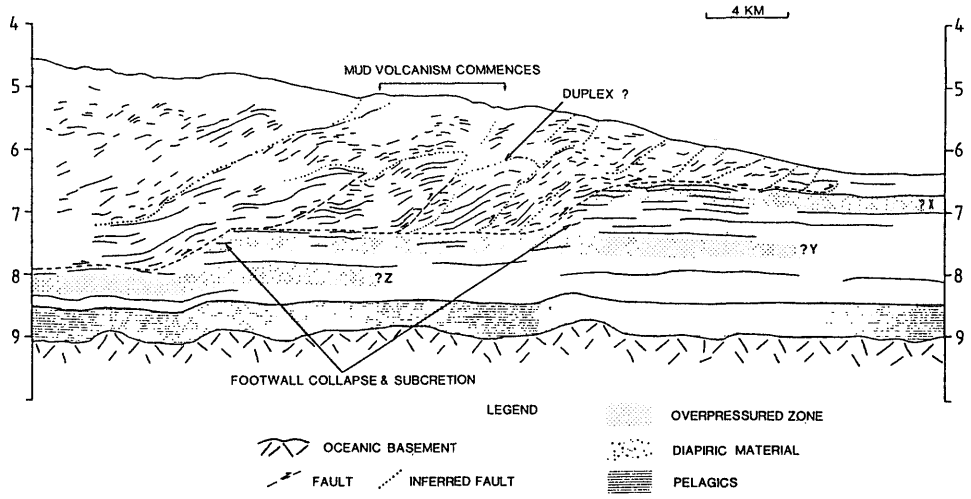

Fig. 22 Line drawing of a seismic reflection section of the frontal Barbados Ridge prism at latitude 13° 20′N (after Brown and Westbrook, 1988). The upper part of trench-filled section is offscraped in front of the prism, while the lower part is underplated at the base of the prism. Note that an underplated section of a horizon X is successively truncated by landward-dipping imbricate thrusts at larger spacing interval than the frontal thrusts at the toe. These truncations may correspond to the sole thrusts of thrust sheets in the Inuyama Sequence.

that (1) a progressive deformation of formation of duplexes below the intrasheet detachment took place in association with south-verging thrusting, and (2) duplex structures are crosscut by a series of low-angle thrusts, the basal one of which correlates with a sole thrust of Sheet 4. The cross relationship between a duplex structure and a sole thrust indicates that the formation of duplex was followed by stacking along sole thrusts. Hence, sole thrusts are not regarded as in-sequence thrusts, but a kind of out-of-sequence thrusts.

The other structural features of sole thrusts are summarized as follows: (1) sole thrusts were rooted into a basal decollement, (2) the attitude of sole thrusts is generally consistent with a homoclinal structure within the upper sheet of each thrust sheet as shown in Fig. 6, and (3) a series of sole thrusts displays flat-ramp-flat structures in Fig. 6. The first two features imply that sole thrusts were generated by reactivation of preexisting thrusts such as in-sequence thrusts and a basal decollement along their almost entire lengths. The last feature suggests that a series of sole thrusts were developed sequentially seaward.

According to classifications of out-of-sequence thrusts by Morley (1988), the sole thrust correlates approximately with an end member of out-of-sequence thrusts, an older in-sequence thrust which is reactivated along their entire length. Hence, sole thrusts of thrust sheets differ from out-of-sequence thrusts in the out-of-sequence thrust zone of active prisms. I call the sole thrusts 'later-stage imbricate thrusts' hereafter.

Recent studies of active prisms indicate that underplating occurs not only in the out-of-sequence thrust zone, but also in the imbricate thrust zone (e.g. Westbrook and Smith, 1983; Kagami, 1985; Brown and Westbrook, 1988; Taira *et al.*, 1988). Among these sections, a seismic profile section from the Barbados Ridge Complex, as shown in Fig. 22 (after Brown and Westbrook, 1988), offers the best clear structural section that implies the underplating of a turbidite sequence and hemipelagite, and associated structural style. This seismic profile suggests that underplated section was progressively stacked by the reactivation of some in-sequence thrusts along their entire length and further extensions to the basal decollement. Structural features of this seismic profile section and its kinematics offer a modern analog of underplating and later-stage imbricate thrusting in the Inuyama Sequence, as illustrated in Fig. 21a. Thrusting along the sole thrust of thrust sheets is likely to lead to shortening and thickening of strata within the upper sheet in association with reactivation of in-sequence thrusts which link the overlying sole thrust to the intrasheet detachment.

In summary, this study offers a deformation process of four-stage for the Inuyama Sequence in the context of structural evolution of the accretionary prism, ranging from the imbricate thrust zone to the frontal out-of-sequence thrust zone (Fig. 21a). (1) The stratigraphic section above the decollement was offscraped by in-sequence thrust faulting with forward propagation in the frontal part of the prism. This offscraping process was followed by (2) underplating of hemipelagic and pelagic intervals to the base of the prism, which formed duplex structures with fault-related folds. This deformed section got a secondary stacking by (3) later-stage imbricate thrusting due to reactivation of some in-sequence thrusts and their extension to the decollement, resulting in the formation of a series of regional-scale thrust sheets. These three stages of deformation process successively took place in the imbricate thrust zone. Finally (4) these imbricated thrust sheets were uplifted over a younger accreted section by out-of-sequence thrusting, leading to substantial thickening of the prism in the out-of-sequence thrust zone.

7. Conclusions

Structural study of the Inuyama Sequence in the Mino-Tamba Belt, central Japan demonstrates accretionary processes of offscraping, underplating and out-of-sequence thrusting. Kimura and Hori (1993) described the structural features of the Inuyama Sequence as follows: 1) the Inuyama Sequence is characterized by the S-verging imbricate fan system of the thrust sheets having oceanic plate stratigraphy, which are subdivided into two lithotectonic units separated by an intrasheet detachment zone, and 2) F_1 mesoscopic folds in ribbon chert are closely related to thrusting, and 3) the offscraping accretionary process followed by down-stepping of the decollement and out-of-sequence thrusting. This study further demonstrates the structural evolution of accretionary process as the following.

(1)The lower sheet of a thrust sheet, which is below the intrasheet detachment, displays a forward-dipping duplex overprinted by recumbent folding and out-of-sequence thrusting and other type of large scale structure such as the forward limb of a fault-bend fold or a antiformal stack.

(2)The sole thrust of the Inuyama Sequence with tectonic melange zone was activated as out-of-sequence thrusting.

(3)Slip vectors of thrusting from major thrust faults at eight localities were measured using the pitch of slickenlines, asymmetric shear fabrics, drag folds and a mesoscale hinterland-dipping duplex. The resulting slip vectors trend between SSE and SSE with respect to the N60° E regional trend of the Inuyama Sequence. This direction is consistent with those derived from mesoscopic F_1 folds reported by Kimura and Hori (1993).

(4)The structural model of the overall accretion of the Inuyama Sequence, which is improved from the model presented by Kimura and Hori (1993), is characterized by a four-stage deformation process consisting of in-sequence thrusting, underplating, later-stage imbricate thrusting and out-of-sequence thrusting, ranging from the imbricate thrust zone to the frontal part of the out-of-sequence thrust zone in active accretionary prisms.

Acknowledgments I thank Prof. Tsunemasa Shiki, Prof. Kiyotaka Chinzei (Kyoto University) and also Prof. Yujiro Ogawa (Tsukuba University) for many helpful discussions and encouragement, and also Dr. Aslam Awan (Quaid-I-Azam University) and Dr. Paul Crenna (Oregon State University) for useful comments on the manuscript.

References

Adachi, M. (1982) Some considerations on the *Mirifusus baileyi* assemblage in the Mino terrane, central Japan. *News Osaka Micropaleontologists Spec. Vol.*, no.5, 211-255**.

Adachi, M. (1988) Further study on the Sakahogi conglomerate and surrounding Mesozoic strata in the southern Mino Terrane, Japan. *Bull. Mizunami Fossil Mus.*, **14**, 113-128**.

Aoki, Y., Tamano, T. and Kato, S. (1982) Detailed structure of the Nankai Trough from migrated seismic sections. *In* Watkins, J. S. and Drake, C. L., eds., *Studies in continental margin geology*. Amer. Assoc. Petrolm Geol. Mem., **34**, 309-322.

Boyer, S. E. and Elliott, D. (1982) Thrust systems. *Bull. Amer. Ass. Petrol. Geol.*, **66**, 1196-1230.

Brown, K., Mascle, A. and Behrmann, J. H. (1990) Mechanisms of accretion and subsequence thickening in the Barbados Ridge accretionary complex : balanced cross sections across the wedge toe. *Proc. ODP, Scientific Results*, **110**, 209-227.

Brown, K. and Westbrook, G. K. (1988) Mud diapirism and subcretion in the Barbados ridge accretionary complex : the role of fluids in accretionary processes. *Tectonics*, **7**, 613-640.

Byrne, T. (1984) Early deformation in melange terranes of the Ghost Rocks Formation, Kodiak Islands, Alaska. *Spec. Pap. Geol. Soc. Amer.*, **198**, 21-51.

DiTullio, L. and Byrne, T. (1990) Deformation paths in the shallow levels of an accretionary prism : the Eocene Shimanto belt of southwest Japan. *Bull. Geol. Soc. Amer.*, **102**, 1420-1438.

Fisher, D. and Byrne, T. (1987) Structural evolution of underthrusted sediments, Kodiak Islands, Alaska. *Tectonics*, **6**, 775-793.

Hashimoto, M. and Saito, Y. (1970) Metamorphism of Paleozoic greenstones of the Tamba Plateau, Kyoto Prefecture. *J. Geol. Soc. Japan*, **76**, 1-6.

Hori, R. (1986) *Parahsuum simplum* Assemblage (Early Jurassic radiolarian assemblage) in the Inuyama area, central Japan. *News Osaka Micropaleontologists, Spec. Vol.*, no.7, 45-52.**

Hori, R. (1988) Some characteristic radiolarians from Lower Jurassic bedded cherts of the Inuyama area, southwest Japan. *Trans. Proc. Palaeont. Soc. Japan, New Ser.*, **151**, 543-563.

Hori, R. (1990) Lower Jurassic radiolarian zones of southwest Japan. *Trans. Proc. Paleont. Soc. Japan, New Ser.*, **159**, 562-586.

Ichikawa, K. (1990) Pre-Cretaceous terranes of Japan. *In* Ichikawa, K., Mizutani, S., Hada, S., and Yao, A. eds., *Pre-Cretaceous Terranes of Japan*. Publication of IGCP Project No. 224 : Pre-Jurassic Evolution of Eastern Asia, 1-11.

Kagami, H. (1985) The accretionary prism of the Nankai Trough off Shikoku, Southwest Japan. *Initial Repts. DSDP*, Washington (U.S. Govt. Printing Office), **87**, 941-953.

Kagami, H., Shiono, K. and Taira, A. (1983) Subduction of plate at the Nankai Trough and formation of accretionary prism. *Kagaku*, **51**, 429-438.*

Kanmera, K. (1980) Geologic structure and its tectonic history. *In* Kanmera, K., Hashimoto, M. and Matsuda, T., eds., *Geology of Japan*, **15**, Iwanami-shoten, Tokyo, 325-350.*

Kano, K., Nakaji, M. and Takeuchi, S. (1991) Asymmetrical melange fabrics as possible indicators of the convergent direction of plates : a case study from the Shimanto Belt of the Akaishi Mountains, central Japan. *Tectonophysics*, **185**, 375-388.

Kimura, G. and Mukai, A. (1991) Underplating units in an accretionary complex : melange of the Shimanto Belt of eastern Shikoku, Southwest Japan. *Tectonics*, **10**, 31-50.

Kimura, K. (1993) Sandstone dikes and their tectonics of Jurassic accretionary complexes. *Monthly Chikyu, Spec. Vol.*, no.8, 204-210*.

Kimura, K. and Hori, R. (1993) Offscraping accretion of Jurassic chert-clastic complexes in the Mino-Tamba Belt, central Japan. *J. Struct. Geology*, **15**, 145-161.

Kimura, K., Makimoto, H. and Yoshioka, T. (1989) *Geology of the Ayabe district*. With Geological Sheet Map at 1 : 50,000, Geol. Surv. Japan, 104p.

Kondo, N. and Adachi, M. (1975) Mesozoic strata of the area north of Inuyama, with special reference to the Sakahogi conglomerate. *J. Geol. Soc. Japan*, **81**, 373-386.**

Matsuda, T. and Isozaki, Y. (1991) Well-documented travel history of Mesozoic pelagic chert in Japan : from remote ocean to subduction zone. *Tectonics*, **10**, 475-499.

Matsuda, T., Isozaki, Y. and Yao, A. (1981) Mode of occurrence of Triassic and Jurassic rocks in Inuyama area, Mino belt. *Proc. Kansai Branch Geol. Soc. Japan*, **88**, 5.*

Matsushita, S. (1953) *Regional Geology of Japan, Kinkichiho 1st ed.* Asakura-shoten, Tokyo, 293p.*

McClay, K. R. and Insley, M. W. (1986) Duplex structures in the Lewis thrust sheet, Crowsnest Pass, Rocky Mountains, Alberta, Canada. *J. Struct. Geol.*, **8**, 911-922.

Mizutani, S. (1964) Superficial folding of the Paleozoic system of central

Japan. *J. Earth. Sci. Nagoya Univ.*, **12**, 17-83.

Mizutani, S. (1990) Mino Terrane. *In* Ichikawa, K., Mizutani, S., Hada, S. and Yao, A. eds., *Pre-Cretaceous Terranes of Japan*. Publication of IGCP Project No. 224 : Pre-Jurassic Evolution of Eastern Asia, 121-135.

Mizutani, S. and Koike, T. (1982) Radiolarians in the Jurassic siliceous shale and in the Triassic bedded chert of Unuma, Kagamigahara City, Gifu Prefecture, central Japan. *News Osaka Micropaleontologists. Spec. Vol.*, **5**, 117-134.**

Moore, G. F., Shipley, T. H., Stoffa, P.L., Karig D. E., Taira, A., Kuramoto, S., Tokuyama, H. and Suyehiro, K. (1990) Structure of the Nankai Trough accretionary zone from multichannel seismic reflection data. *J. Geophys. Res.*, **95**, 8753-8765.

Moore, J. C., Cowan, D. S. and Karig, D. E. (1985) Structural styles and deformation fabrics of accretionary complexes. *Geology*, **13**, 77-79.

Moore, J. C., Watkins, J. S., McMillen, K. J., Bachman, S. B. and Lundberg, N. (1982) Geology and tectonic evolution of a juvenile accretionary terrane along a truncated convergent margin : synthesis of results from Leg 66 of the Deep Sea Drilling Project, southern Mexico. *Geol. Soc. Amer. Bull.*, **93**, 847-861.

Morley, C. K. (1988) Out-of-sequence thrusts. *Tectonics*, **7**, 539-561.

Murata, A. (1991) Duplex structures of the Uchinohae Formation in the Shimanto Terrane, Kyushu, Southwest Japan. *J. Geol. Soc. Japan*, **97**, 39-52.

Needam, D. T. and Mackenzie, J. S. (1988) Structural evolution of the Shimanto Belt accretionary complex in the area of the Gokase River, Kyushu, SW Japan. *J. Geol. Soc. London*, **145**, 85-95.

Otofuji, Y., Matsuda, T. and Nohda, S. (1985) Paleomagnetic evidence for the Miocene counterclockwise rotation of Northeast Japan rifting process of the Japan Arc. *Earth Planet. Sci. Letters*, **75**, 265-277.

Otsuka, T. (1988) Paleozoic-Mesozoic Sedimentary complex in the eastern Mino Terrane, central Japan and its Jurassic Tectonism. *J. Geosci. Osaka City Univ.*, **31**, 63-122.

Platt, J. P., Leggett, J. K. and Alam, S. (1988) Slip vectors and fault mechanics in the Makran accretionary wedge, southwest Pakistan. *J. Geophs. Res.*, **93 B7**, 7955-7973.

Sample, J. C. and Fisher, D. M. (1986) Duplex accretion and underplating in an ancient accretionary complex, Kodiak, Islands, Alaska. *Geology*, **14**, 160-163.

Shipley, T. H., Moore, G. F., Bangs N. L., Moore, J. C., and Stoffa, P. L. (1994) Seismically inferred dilatancy distribution, northern Barbados Ridge decollement : implications for fluid migration and fault strength. *Geology*, **22**, 411-414.

Silver, E. A., Ellis, M. J., Breen, N. A. and Shipley, T. H. (1985) Comments on the growth of accretionary wedges. *Geology*, **13**, 6-9.

Taira, A., Katto, J., Tashiro, M., Okamura, M. and Kodama, K. (1988) The Shimanto Belt in Shikoku, Japan - evolution of Cretaceous to Miocene accretionary prism -. *Modern Geology*, **12**, 5-46.

Taira, A., Hill I., Firth, J., Berner, U., Bruckmann, W. *et al.* (1992) Sediment deformation and hydrogeology of the Nankai Trough accretionary prism : synthesis of shipboard results of ODP Leg 131. *Earth Planet. Sci. Letters*, **109**, 431-450.

Tokunaga, T. (1992) Duplexing and intraprism deformation of the Paleogene Shimanto Supergroup in western Shikoku, Southwest Japan. *Tectonics*, **11**, 1168-1179.

Wakita, K. (1988) Origin of chaotically mixed rock bodies in the Early Jurassic to Early Cretaceous sedimentary complex of the Mino terrane, central Japan. *Bull. Geol. Surv. Japan*, **39**, 675-757.

Wakita, K., Harayama, S., Kano, K., Mimura, K. and Sakamoto, T. (1992) *Geologic map of Japan 1:200,000, Gifu*. Geological survey of Japan.

Watkins, J. S., Moore, J. C., *et al.* (1982) *Initial reports of the Deep Sea Drilling Project*. Washington, D.C., U.S. Government Printing Office, **66**, 864 p.

Westbrook, G. K., Ladd, J.W., Buhl, P.,

Bangs, N. and Tiley, G. J. (1988) Cross section of an accretionary wedge: Barbados Ridge complex. *Geology*, **16**, 631-635.

Westbrook, G. K. and Smith, M. J. (1983) Long decollements and mud volcanoes : evidence from the Barbados Ridge complex for the role of high pore-fluid pressure in the development of an accretionary complex. *Geology*, **11**, 279-283.

Yamada, N. and Wakita, K. (1990) *Geologic map of Japan 1:200,000, Iida*. Geological survey of Japan.

Yao, A., Matsuda, T. and Isozaki, Y. (1980) Triassic and Jurassic radiolarians from the Inuyama area, central Japan. *J. Geosci. Osaka City Univ.*, **23**, 135-155.

*In Japanese. **In Japanese with English abstract.

Received March 6, 1997
Accepted June 18, 1997

付加体における剝ぎ取り，底付け，アウトオブシークエンススラスト過程：中部日本，美濃-丹波帯の例

木村克己

要　旨

美濃地域に分布する美濃-丹波帯の犬山シークェンスについて，Kimura and Hori(1993)の研究を基礎に，マスターソールスラスト，デュープレックス構造の特徴と運動像の解析を新たに行い，付加過程における2つのタイプのアウトオブシークェンススラストの役割を加えた，比較的浅いレベルでの付加過程のモデルを示した．

犬山シークェンスには，規模や形態の異なる5つのタイプのスラスト，すなわち，マスターソールスラスト，規模の異なる2種類の覆瓦スラスト，イントラデタッチメント，デュープレックスが識別される．

マスターソールスラストは犬山シークェンスの基底を切るもので最大規模であり，美濃-丹波帯を構成するいくつかの堆積岩コンプレックスの境界をなすスラストのひとつである．同スラストは高角度に傾斜する上盤・下盤の構造を低角度に切る．これに収れんする覆瓦スラストは，広域的規模の6枚のスラストシートからなる南フェルゲンツの覆瓦構造を形成する．各スラストシートは，前期三畳紀から後期ジュラ紀にわたる海洋プレート層序，すなわち，下部から上部へ，珪質粘土岩，層状チャート，珪質泥岩，粗粒砕屑岩の各層から構成される．これら各スラストシート内部には，珪質泥岩の層準にイントラシートデタッチメントが発達しており，これによって，主に粗粒砕屑岩からなる上部シートと，主に珪質粘土岩・層状チャート・珪質泥岩からなる下部シートに二分される．上部シートは変形が弱く同斜構造を示し，イントラシートデタッチメントから派生する覆瓦スラストの存在で，下部シートは小褶曲を伴うデュープレックス構造でそれぞれ特徴づけられる．これらすべてのスラストのスリップベクトルは，犬山シークェンスのN60°Eの一般走向に対してほぼ直交する南南東から南南西の方向を示す．

以上の構造形態と運動像に基づいて4つのステージからなる付加過程を導きだすことができる．(1)デコルマンが初めに珪質泥岩の層準に発生し(イントラデタッチメントに相当)，デコルマンの層準より上位の地層は，付加体のフロントで順次前方に発達するスラストにより切られて短縮・付加され，覆瓦ファン構造をなす．(2)デコルマン下位の地層はデュープレックス構造をなして底づけ付加される．(3)初期の覆瓦スラストの一部が再活動しさらに下方へ延長する結果，広域的規模のスラストシートからなる覆瓦構造が形成される．(4)低角度の後期アウトオブシークェンススラストが付加体内の構造を切って，付加体は著しく厚みを増す．同スラストは犬山シークェンスのマスターソールスラストに相当する．